SYNTHESIS AND CHARACTERIZATION OF SHAPE MEMORY POLYURETHANE FOR BIOMEDICAL APPLICATIONS

by

Serap Başkır

BS., in Chemistry, Boğaziçi University, 2015
MS., in Chemistry, Boğaziçi University, 2017

Submitted to the Institute of Biomedical Engineering
in partial fulfillment of the requirements
for the degree of
Doctor
of
Philosophy

Boğaziçi University
2024

SYNTHESIS AND CHARACTERIZATION OF SHAPE MEMORY POLYURETHANE FOR BIOMEDICAL APPLICATIONS

APPROVED BY:

Prof. Dr. Bora Garipcan ..... (Thesis Advisor)

Prof. Dr. Esin Öztürk Işık .....

Assist. Dr. Banu İyisan .....

Assoc. Dr. Emre Tekay .....

Prof. Dr. Lokman Uzun .....

DATE OF APPROVAL: 22 November 2024

"To myself, for the quiet strength that carried me through storms, the unyielding hope that lit my path in darkness, and the resilience that turned pain into growth... Let this be the testament of the person I have become and the journey I have embraced. May it forever remind me that even in solitude, I was enough."

ACADEMIC ETHICS AND INTEGRITY STATEMENT

I, Serap Başkır, hereby certify that I am aware of the Academic Ethics and Integrity Policy issued by the Council of Higher Education (YÖK) and I fully acknowledge all the consequences due to its violation by plagiarism or any other way.

Name :

Signature:

Date:

ABSTRACT

SYNTHESIS AND CHARACTERIZATION OF SHAPE MEMORY POLYURETHANE FOR BIOMEDICAL APPLICATIONS

Incorporation of shape memory polymers into biomedical devices is an attractive option due to their notable advantages of low cost, biocompatibility, tunable degradability, patient specific design, and adjustable mechanical and thermal properties. Shape memory polyurethanes are particularly attractive due to their extensive temperature range for shape recovery as well as the ability to fine-tune the glass transition temperature. This study aimed to synthesize an SMPU using Glycerol as chain extender with a glass transition temperature within a suitable temperature range for biomedical applications. The results showed that the triggering temperatures for the synthesized samples changes between 63.95 °C and 88.21 °C. Shape memory properties were investigated for the temperature range of 40 °C and 75 °C. Shape recovery times were found to be substantially with increasing temperature with 102 seconds at 40 °C and ∼1 second at 75 °C. Shape fixity and shape recovery rates for the same temperature ranges were 77.8 % & 85.6 % at 40 °C and 100 % & 100 % for 75 °C. Cytotoxicity assay indicate promising biocompatibility of the synthesized material for biomedical purposes. Overall, the synthesized polymers were found to be a potential candidate for biomedical applications such as stents, aneurysm filling or occlusion devices.

Keywords: Shape Memory Polyurethane, SMPU, Glycerol.

ÖZET

BİYOMEDİKAL UYGULAMALAR İÇİN ŞEKİL HAFIZALI POLİÜRETAN SENTEZİ VE KARAKTERİZASYONU

Şekil hafızalı polimerlerin biyomedikal cihazlara dahil edilmesi, düşük maliyet, biyouyumluluk, ayarlanabilir bozunabilirlik, hasta spesifik tasarım ve ayarlanabilir mekanik ve termal özellikler gibi önemli avantajlarıdan dolayı çekici bir seçenektir. Şekil hafızalı poliüretanlar, geniş şekil geri kazanım sıcaklık aralığı ve cam geçiş sıcaklığını ince ayar yapabilme yeteneği nedeniyle özellikle caziptir. Bu çalışma, biyomedikal uygulamalar için uygun bir sıcaklık aralığında camsı geçiş sıcaklığına sahip bir şekil hafızalı poliüretan (SMPU) sentezlemeyi amaçlamıştır. Sonuçlar, sentezlenen örneklerin tetikleyici sıcaklıklarının 63,95 °C ile 88,21 °C arasında değiştiğini göstermiştir. Şekil hafızası özellikleri, 40 °C ile 75 °C arasındaki sıcaklık aralığı için incelenmiştir. Şekil geri kazanım sürelerinin, sıcaklık arttıkça önemli ölçüde azaldığı bulunmuştur; 40 °C'de yaklaşık 102 saniye, 75 °C'de ise yaklaşık 1 saniye olarak ölçülmüştür. Aynı sıcaklık aralığında şekil sabitleme ve şekil geri kazanım oranları ise 40°C'de %77,8 ve %85,6, 75 °C'de ise %100 ve %100 olarak tespit edilmiştir. Sitotoksisite testi, sentezlenen malzemenin biyomedikal uygulamalar için umut verici bir biyouyumluluk sergilediğini göstermiştir. Genel olarak, sentezlenen polimerlerin stentler, anevrizma doldurma cihazları veya tıkanma cihazları gibi biyomedikal uygulamalar için potansiyel bir aday olduğu bulunmuştur.

Anahtar Sözcükler: Şekil hafızalı poliüretan, Gliserol, Camsı geçiş sıcaklığı, Şekil Geri Kazanımı

TABLE OF CONTENTS

. iii
ACADEMIC ETHICS AND INTEGRITY STATEMENT iv
ABSTRACT v
ÖZET vi
LIST OF FIGURES ix
LIST OF TABLES x
LIST OF SYMBOLS xi
LIST OF ABBREVIATIONS xii
1. BACKGROUND INFORMATION 1
1.1 Introduction 1
1.2 Shape Memory Polyurethane in Biomedical Applications 3
1.2.1 Biocompatibility 5
1.2.2 Degradation 6
1.2.3 Adjustable Mechanical Properties 8
1.2.4 Triggering Mechanisms 9
1.2.5 Medical Device Designed with Shape Memory Polymers 10
1.3 List of publications produced from the thesis 13
1.4 Overview of thesis 13
2. SHAPE MEMORY POLYURETHANE SYNTHESIS BY USING GLYCEROL AS CHAIN EXTENDER FOR BIOMEDICAL APPLICATIONS 14
2.1 Introduction 14
2.2 Materials and Methods 16
2.2.1 Materials 16
2.3 Characterization of the SMPU samples 18
2.3.1 Thermogravimetric Analysis 18
2.3.2 Differential Scanning Calorimetry 18
2.3.3 Fourier Transform Infrared Spectroscopy 18
2.3.4 Dynamic Mechanical Analysis 18
2.3.5 Shape Memory Behaviour 19

2.3.6 Cell Culture and MTT Cytotoxicity Assay 19
2.4 Results and Discussion 20
2.4.1 Thermogravimetric analysis 20
2.4.2 Differential Scanning Calorimetry 22
2.4.3 Fourier Transform Infrared Spectroscopy 23
2.4.4 Dynamic Mechanical Analysis 25
2.4.5 Shape Memory Properties 28
2.4.6 Cell culture and MTT cytotoxicity assay 30
3. DISCUSSION 32
REFERENCES 35

LIST OF FIGURES

Figure 1.1	Schematic representation of a 1-way dual shape memory cycle.	1
Figure 2.1	Schematic representation of the monomers used in the study and the polymer network of synthesized SMPU samples.	17
Figure 2.2	Thermogravimetric analysis (TGA) curves of the 5 SMPU samples.	21
Figure 2.3	Differential Scanning Calorimetry (DSC) thermograms of the 5 SMPU samples.	22
Figure 2.4	Fourier Transform Infrared (FTIR) spectra of the 5 SMPU samples.	24
Figure 2.5	Dynamic Mechanical Analysis (DMA) of the 5 SMPU samples.	26
Figure 2.6	Shape memory properties of the 5 SMPU samples.	29
Figure 2.7	Permanent, temporary, and recovered shapes.	29
Figure 2.8	Cellular viability of L929 mouse fibroblasts after 24 hours of culture.	31

LIST OF TABLES

Table 1.1	Common components used in the synthesis of SMPU and their application areas in the literature.	4
Table 1.2	Common components used in the synthesis of SMPU and their application areas in the literature (cont.).	5
Table 2.1	Monomer Ratios (moles) of the samples using HDI (Hexamethylene diisocyanate), HPED (N,N,N',N'-Tetrakis (2-hydroxypropyl) ethylenediamine), and GLY (Glycerol).	17
Table 2.2	Thermal degradation profiles of the 5 SMPU samples from thermogravimetric analysis (TGA).	21
Table 2.3	Glass transition Temperatures (T_g) of the 5 SMPU samples from differential scanning calorimetry (DSC) thermograms.	23
Table 2.4	Glass transition Temperatures (T_g) and storage modulus (E') of the 5 SMPU samples from Dynamic Mechanical Analysis (DMA).	26
Table 2.5	Storage modulus (E') and tan δ of the 5 SMPU at 25 °C.	27

LIST OF SYMBOLS

T_g	Glass Transition Temperature
T_m	Melting Temperature
R_f	Shape Fixity Ratio
R_s	Shape Recovery Ratio
ε	Strain
ε_{load}	Strain under Load
$\varepsilon_{recovery}$	Strain under Load
°C	Celcius Degree

LIST OF ABBREVIATIONS

SMP	Shape Memory Polymer
PCL	Poly(ε-caprolactone)
PVA	Poly(lactic acid)
HDI	Hexamethylene diisocyanate
HPED	N,N,N',N' - Tetrakis (2 - hydroxypropyl) ethylenediamine
GLY	Glycerol
FBS	Fetal Bovine Serum
SMPU	Shape Memory Polyurethane
DMEM-F12	Dulbecco's Modified Eagle Medium: Nutrient Mixture F12
TMHDI	Trimethylhexamethylene Diisocyanate
IPDI	Isophorone diisocyanate
PEG	Polyethylene Glycol
HDMI	2-(2'-hydroxyphenyl)-3,3'-dimethylindole
pH	Power of Hydrogen
PLLA	Poly-L-Lactic Acid
PLGA	Poly(lactic-co-glycolic) Acid
PHBV	Poly(3-hydroxybutyrate-co-3-hydroxyvalerate)
TEA	Triethanolamine
SMC	Shape Memory Ceramic
SMA	Shape Memory Alloy
TGA	Thermogravimetric Analysis
DSC	Differential Scanning Calorimetry
FTIR	Fourier Transform Infrared Spectroscopy
DMA	Dynamic Mechanical Analysis
MTT	3-(4,5-Dimethylthiazol-2-yl)-2,5-Diphenyltetrazolium Bromide
MPa	Mega Pascal

1. BACKGROUND INFORMATION

1.1 Introduction

Shape memory polymers (SMPs) refer to polymeric materials that have more than one shape (e.g., permanent shape and temporary shape(s)) and that have the ability to alter between these shapes with stimuli. Permanent shape is designed in the initial process of the material and temporary shape is designed by mechanical shape deformation and fixation under a thermal transition. This thermal transition may correspond to the glass transition temperature (T_g) in the case of amorphous polymers, chemically crosslinked thermosets, and physically crosslinked thermoplastics, or the melting temperature (T_m) in semi-crystalline polymers, chemically crosslinked rubbers, and physically crosslinked polymers [1],[2],[3] Returning to permanent shape is achieved by applying external stimuli (e.g., temperature, pH, light, moisture, magnetic field) to the material in temporary shape. Thus, the general schematic for the shape memory cycle of an SMP is given in Figure 1.1.

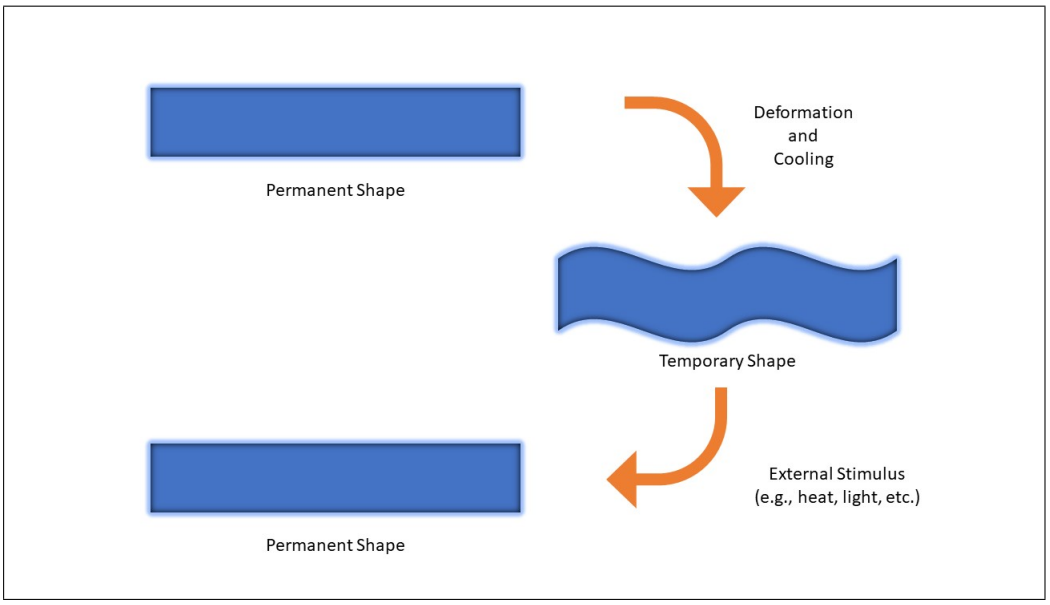


Figure 1.1 Schematic representation of a 1-way dual shape memory cycle.

SMPs can be categorized with respect to the number of shapes they can mem-

orize and with respect to their ability to transition between these shapes. In terms of the number of shapes memorized, the common type of SMPs is called Dual SMPs, where the SMP has one permanent shape, one temporary shape, and one transition temperature (e.g., glass transition, melting) for shape transition. However, it is possible for SMPs to have more than two shapes, with each additional shape generally programmed with distinct thermal transition temperatures or with a broad transition temperature, which are called Multiples SMPs [3],[4],[5]. In terms of the ability to transition between shapes, the common type of SMPs is called one-way SMP, where shape recovery from temporary shape to permanent shape with an external stimulus is possible, but a following shape change from permanent shape back to temporary shape is not. On the other hand, two-way SMPs have the capability to interchange between shapes with appropriate stimuli [3],[4],[5]. Typical procedure for shape programming of a dual-shape one-way SMP [3],[6],[7]: (1) SMP is heated above transition temperature (e.g., $T_x > T_g$ or $T_x > T_m$) and held isothermally. (2) External force applied to deform into temporary shape. (3), for the fixation of temporary shape, SMPs is cooled down below transition temperature (e.g., $T_x < T_g$ or $T_x < T_m$) and, the external load is removed, and held isothermally. (4) For shape recovery, SMP is heated back above transition temperature. Consecutively, the shape-change behavior of SMPs is assessed with two parameters [8], the shape fixity ratio R_f indicating the ability to maintain an imposed mechanical deformation after the load is removed, and shape recovery ratio R_r, indicating the ability to recover permanent shape. The equations for these two parameters are as follows [5]:

$$R_f(\%) = \frac{\epsilon}{\epsilon_{load}} \cdot 100 \tag{1.1}$$

$$R_s(\%) = \frac{\epsilon - \epsilon_{recovery}}{\epsilon_{recovery}} \cdot 100 \tag{1.2}$$

Where ε is strain, ϵ_{load} is strain under load, and $\epsilon_{recovery}$ is the strain under recovery.

Initial studies on SMPs were patents for dental materials and heat-shrinkable

tubing and films [1],[9], where the practical utilization of SMPs were priority. In the last decades, SMPs gained more traction in academic field with the aim to understand the thermomechanical properties of such materials and characteristics of the "shape-change mechanism" [1],[9]. In the literature, many polymers have been studied to show shape memory behavior and used to design SMPs [1],[9],[10],[11], with more common ones among these being epoxy based [10],[11], Poly(lactic acid) (PLA) based, Poly(ε-caprolactone) (PCL) based , polyurethane (PU) based [12],[13],[14], and Poly(vinyl alcohol) (PVA) based SMPs [12]. With the technological and scientific advancements, SMPs became desirable materials in various fields like aerospace engineering [15],[16],[17], soft robotics, sensors [18][19],[20], 4D printing, smart textiles [21], surface patterning [22]. In recent years, potential of SMPs also has been studied in biomedical field due to their properties like easy processability, low cost, light weight, adjustable stiffness, biocompatibility [23], and tunable biodegradability with controllable degradation rate (depending on the application). Such advantages made SMPs favourable materials in next-generational biomedical devices [23],[24],[25]. Among these polymers that shows shape memory effect, polyurethane is a favourable material for biomedical field [8],[26] as it is already used in medical devices [27]. It inherently has hard and soft segments, and desired working temperature range and material characteristics can be achieved by controlling the hard & soft segment ratio [8]. Polyurethane has high strain recovery, can be found in different forms, and its color and transparency can be decided by its constituents [8]. These properties help to design related shape memory properties (e.g., glass transition temperature or melting temperature, shape recovery rate and external stimuli) for biomedical applications.

1.2 Shape Memory Polyurethane in Biomedical Applications

Polyurethanes are generally composed of a diisocyanate, a macrodiol), and a chain extender (diol or diamine) [27],[28]. Segmented polyurethane can be synthesized with either (1) pre-polymer method where diisocyanate is reacted with macrodiol to form a pre-polymer which is later reacted with chain extender, or with (2) one-shot method where all monomers are reacted once [27]. Consecutively, polyurethanes are

composed of tangled long linear polymer chains alternatively connected hard segments (formed by diisocyanate and chain extender) and soft segments (formed by macrodiol and diisocyanate) [26],[29]. The common monomers used in the synthesis of SMPU for biomedical studies is given in table 1.1 and table 1.2. The shape memory behaviour of SMPU is achieved by these hard segments that provide the mechanical strength for permanent shape and soft segments that provide the transition properties to attain and recover from temporary shape [8][29].

Table 1.1
Common components used in the synthesis of SMPU and their application areas in the literature.

Ref	**Hard Segment**	**Soft Segment**	**Chain Extender**	**Application Field**	**Type**
[30][31][32][33] [34][35][36][37] [38][39][40] [41] [42]	HDI	HPED	TEA	Cardiovascular Applications	Foam Film Foam/Film
[43][44] [45][46]	HDI	PLLA	BDA	Biomedical Applications Tissue Engineering	Film
[43][44][47] [45][46]	HDI	PDLLA	PP	Biomedical Applications Tissue Engineering	Film
[48][49][50] [51]	HDI	PCL	BD	Biomedical Applications Tissue Engineering Drug Delivery	Film Electrospun Fiber
[52]	HDI	PCL	PP	Biomedical Applications	Film
[53]	HDI	PLLA	PCL	Biomedical Applications	Film
[54]	HDI	PPG	PEG	Biomedical Applications	Film
[30][34][35] [42]	TMHDI	HPED	TEA	Cardiovascular Applications	Foam Foam/Film
[30][34] [42]	IPDI	HPED	TEA	Cardiovascular Applications	Foam Foam/Film
[50][55][56][57] [58][59]	IPDI	PCL	BD EG	Biomedical Applications Tissue Engineering	Film Scaffold

Table 1.2
Common components used in the synthesis of SMPU and their application areas in the literature (cont.).

Ref	Hard Segment	Soft Segment	Chain Extender	Application Field	Type
[60]		PEG	BD	Biomedical Applications	Film
[61][62][63][64]	MDI	PCL	EG	Biomedical Applications	Film
[65][66]				Cardiovascular Applications	Film
[67][68]			BD	Tissue Engineering	Film
[69]		PEG		Biomedical Applications	Film
[70]	MDI	PTMEG	BD	Tissue Engineering	Scaffold
[71][72]	MDI	PCL	DTH	Tissue Engineering	Film
[71][72]	HDI	PEG			
[73]	MDI	PLA	PCL	Biomedical Applications	Film
[51]	HDI	PEG	BD	Tissue Engineering Drug Delivery	Film
[51][57]	MDI/TDI	PLA		Biomedical Applications	Film
[74]	TDI	PCL	EG	Biomedical Applications	Film

1.2.1 Biocompatibility

Biocompatibility is crucial for biomedical applications where the desired body response is required for optimum device performance & treatment and patient recovery. This desired response may vary from no immune response or inflammation to promoting cell adhesion and cell growth, depending on the application. The assessment of biocompatibility is performed via in-vitro and in-vivo tests. Initial assessment of biocompatibility is done with in-vitro tests like cell viability [50],[54], cell cytotoxicity [47],[57],[61],[62],[64],[69], and proliferation tests [50] as these tests are simple and cost efficient. Nonetheless, these tests enable the examination of cell-material interactions, cytotoxicity, and cell proliferation, providing a basic insight without the complexities of in-vivo tests. Consecutively, varying in-vitro tests are utilized in studies according to the needs of their field and application. For cardiovascular applications, priority is the blood-material interactions, hence cytotoxicity [32],[40],[42] and platelet acti-

vation/adhesion [38] tests may be enough for the initial evaluation of the material. Whereas for tissue engineering, cell and metabolic activity is priority with tests like cell adhesion [51],[58],[59], osteogenic differentiation and activity [58], antibacterial activity [59],[66] are common. In-vivo tests, on the other hand, require expertise, and time consuming through the whole process. In-vivo testing presents conditions that cannot be accurately simulated by and provides data that cannot be acquired in-vitro. Hence, it is vital when the study requires a deep understanding of the material within a complex biological and physiological context such as short-term and long-term biocompatibility and adverse effects, systemic interactions of body/organs and materials, and effects on metabolism. Consecutively, in-vivo tests are performed in studies that went deeper into the research. Xie et. al [47] studied in-vivo toxicology of their material by haematological, biochemical, and histological analyses and showed that the material had no apparent effect in terms of toxicity, side effects, or organ functionality. Tissue regeneration capacity of SMPU was studied in-vivo by several studies [58],[68], showing increased bone tissue regeneration with functionalized SMPUs.

1.2.2 Degradation

Degradation is often considered a drawback for SMPs, however for the biomedical field this property becomes a critical design characteristic. Primarily, controllable degradation and biodegradability eliminates the additional surgery required for the removal of the implant after treatment. This is particularly advantageous in tissue engineering scaffolds and drug delivery systems where the material degradation rate is designed in accordance with the required treatment period, with the material gradually undergoing enzymatic or hydrolytic degradation and dissipating. Consecutively, the risk of post-operative complications and the overall cost of the treatment can be substantially reduced. The degradation of kinetics in this regard has critical implications: If not tailored properly, it may lead to a cascade of adverse outcomes that comprise both the efficacy of the medical device and patient safety. Fast degradation can lead to the failure of the device, leading to insufficient support or therapy before the healing process is complete. A tissue scaffold degrading too quickly may

induce an inflammatory response [75] or collapse before new tissue is fully formed and undermine tissue regeneration [76],[36]. On the other hand, slow degradation of the SMPU may provoke a prolonged inflammatory response [77] and in some cases stress shielding [76],[36],[78]. In drug delivery systems, improper degradation rates could lead to erratic or sustained release of the therapeutic agent [79]. Moreover, the accumulation of non-degraded polymer fragments could lead to physical obstruction, delayed healing, embolism or thrombosis, especially in cardiovascular applications [80]. Additionally, the presence of durable polymers could interfere with imaging and diagnostic procedures, obscuring the visual field or providing false signals.

Degradation of SMPUs in biomedical applications mainly occurs via hydrolysis and oxidation [81]. Hydrophobicity of the monomers and polymer is a direct way to control degradation. In their study, Singhal et al had different rates of mass loss with different hard segment monomer/isocyanate compositions [34]. Their results showed that the degradation rate decreased with substituting HDI with TMHDI and IPDI, with the change associated with the more hydrophobic nature of the TMHDI and IPDI monomers. Similar results were shown [42] where IPDI was found to be resistant to degradation with respect to HDI. Hydrophobicity of the soft segment also found to affect the degradation rate [53],[71], where among the two SMPUs synthesized with PEG and PCL monomers as soft segment, the SMPU with PEG was shown to have a faster degradation rate [71] due to PEG being more hydrophilic. Overall, the idea is to reduce the water uptake (for especially foams/scaffolds) with the utilization of hydrophobic monomers and reducing exposure of hydrolytically susceptible linkages [38], which can be achieved via hydrophobic of the monomers (as hard & soft segments), molecular weight of the monomers [38], crystallinity of the monomers [34],[51],[49],[69] as well as the hard segment / soft segment ratio [34],[54]. However, there are other cases that can limit the exposure of hydrolyzable end groups and reduce degradation rate. In their study, Sarkar et al showed that a modification in diisocyanate structure results in adverse changes on degradation rate of the polymer. Changing from HDI to HDMI, which is a monomer with a more amorphous structure, amplified the degradation rate in PCL-based SMPU whereas it unexpectedly caused a slower degradation in its PEG-based counterpart. This variance was attributed to the distinct morphologies of these

polyurethanes. In PEG-based polyurethane, a transition from HDI to HMDI yielded a more phase mixed structure that mixed with hydrogen bonding between urethane linkages and the soft segment, consecutively reducing the number of linkages susceptible to hydrolytic degradation.

1.2.3 Adjustable Mechanical Properties

Unlike traditional materials, SMPs can be precisely engineered to exhibit a broad range of mechanical behaviors, allowing them to match the specific requirements of various tissues. This tunability is particularly significant in applications such as tissue engineering, where scaffolds need to mimic the mechanical properties of the native tissue closely [43]. SMPs can transition from a soft, malleable state to a more rigid structure in response to external stimuli, such as temperature changes, which enables dynamic support for regenerating tissues [58].

The ability to adjust mechanical properties allows SMPs to offer more than just structural support. For instance, in applications like bone regeneration, SMPs can be engineered to selectively release growth factors at different stages of the healing process, facilitating the development of new bone tissue in a controlled manner [58], [59]. This property also allows SMPs to be used in the development of patient-specific implants, which can be tailored to the unique anatomical and biomechanical needs of the individual, enhancing both the efficacy of the implant and the overall patient outcomes.

Moreover, SMPs' adjustable mechanical properties are not static but can evolve over time to match the changing requirements of the healing tissue. This dynamic adaptability ensures that the material provides optimal support throughout the different stages of tissue regeneration. For example, SMP-based scaffolds can initially provide a high level of stiffness to support cell attachment and proliferation [70]. As the tissue regenerates and strengthens, the scaffold can become softer, allowing the tissue to take over the mechanical load gradually [45], [46]. This evolution in mechanical

properties is a significant advantage over traditional materials, which typically do not change once implanted.

1.2.4 Triggering Mechanisms

SMPs can respond to triggers such as temperature, light, moisture, and pH changes, allowing them to be used in diverse therapeutic and diagnostic contexts [4]. Temperature is one of the most commonly used triggers for SMPs [57]. For instance, in minimally invasive surgery, SMPs can be inserted into the body in a compact form. Once in place, the natural body heat can trigger the material to expand or change shape, thereby providing necessary structural support or delivering therapeutic agents directly to the targeted area. This characteristic makes SMPs particularly useful in applications like vascular stents or orthopedic implants, where precise deployment and adaptation to the body's conditions are crucial.

In addition to thermal triggering, SMPs can also be activated by light, which offers the advantage of non-invasive control. Light-responsive SMPs can be designed to change shape or release drugs upon exposure to specific wavelengths of light [47]. This property is especially useful in applications like targeted drug delivery systems, where the material can remain inactive until it is exposed to light at the target site, ensuring that the therapeutic agents are released only where needed, thus minimizing side effects and maximizing efficacy.

Moisture and pH are also significant triggers that can be utilized in SMPs, especially in environments where these factors vary naturally, such as within different regions of the body. For example, pH-sensitive SMPs can be used in drug delivery systems [51] that release medication in response to the acidic environment of a tumor or an infected area, ensuring that the treatment is delivered precisely where it is needed. Similarly, moisture-responsive SMPs can be designed to swell or change shape in response to the presence of bodily fluids, making them ideal for applications such as wound healing or tissue scaffolds [67],[68].

Magnetic fields provide a unique, non-invasive triggering method for SMPs [82]. Magnetic-responsive SMPs can be used in a variety of applications, from remotely controlled drug delivery systems to adaptive implants that change shape or stiffness in response to external magnetic fields. This capability allows for real-time adjustments to the material's properties, enabling clinicians to fine-tune treatment protocols during the course of therapy. For instance, in orthopedic applications, magnetic-responsive SMPs could be used to create implants that adjust their mechanical properties based on the patient's activity level or healing progress [52]. This dynamic adjustment helps in maintaining optimal support for healing tissues while reducing the risk of implant failure or the need for additional surgeries.

1.2.5 Medical Device Designed with Shape Memory Polymers

In the recent years, SMPs become a popular option to design biomedical implants instead of shape-memory alloys like Nitinol [25]. Polyurethane (PU) is one of the most attractive polymers that are used to design SMP-based implants. Hard segment and soft segment of PU enables utilization of PU in SMP design, as they provide netpoints and switching segments, respectively. Additionally, it can be synthesized in porous and non-porous forms. Furthermore, due to their inherent biocompatibility and mechanical properties, shape-memory polyurethanes (SMPUs) are highly considered in cardiovascular implant design.

Stents comprise a substantial part of the cardiovascular devices. Depending on the type of stent (e.g. coronary/peripheral or drug eluting/bare metal) [83], the implant may require different properties. In some cases, biodegradability is desired, whereas porosity (and its percentage) may be advantageous or not [84] whereas rapid self-deployment and simple retraction are highly desired. This high diversity of properties is also reflected to the SMP-based implant studies. Controlled deployment and retraction via direct triggering might be essential for accurate treatment. Baer et al [85] designed a SMPU-based stent using a commercially available SMPU. This heat driven stent had favourable mechanical properties and biocompatibility. However, the stent

expansion is observed at 80 °C, which is above the body temperature (37 °C). Bellin et al [86] synthesized a triple shape-memory polymer networks composed of PEG-PCL segments. The idea of triple shape-memory effect is to enable an additional temporary shape for stent removal. However, the prototype showed stent-deployment 40 °C, and stent-removal at 70 °C. Yakacki et al. [87] synthesized a thermally-driven SMP by using tert-butyl acrylate and poly(ethylene glycol) dimethacrylate. They designed a stent with T_g of 55 °C. Yang et al. [88] developed a drug-eluting & biodegradable stent by cross-linking PEG-PCL copolymer (cPEG-PCL). Thermally induced shape recovery is observed above the body temperature (41 °C and 45 °C) with a recovery rate of 10 seconds. However, the stent requires an indirect heating method and shape recovery of the stent is sub-optimal. Additionally, self-expansion is an attractive property for SMP-based stents. One of the first works for biodegradable & self-expanding stents is done by Venkatraman et al [89]. The stent is designed from PLLA+PLGA polymers. By adjusting the ratios, they obtained full expansion at body temperature within 8 minutes. Chen et al. [90] developed a self-expanding stent based on chitosan blended. Expansion time of the stent was around 150 seconds at 37 °C. On the other hand, its shape-memory properties needed improvement. There are also some studies observing relatively fast deployment rates. Xue et al [91] synthesized biodegradable SMP from hyperbranched three-arm poly(ε-caprolactone) (PCL) as switching segment and microbial polyester PHBV as crystallizable hard segment. The stent showed self-expansion in water bath at 37 °C within 25 seconds, but its biocompatibility needed improvement.

Aneurysm treatment is another major concern among cardiovascular diseases. Different types of aneurysms [92],[93] (fusiform aneurysm, wide-necked aneurysm) may require different approaches. This allows utilization of shape-memory polymers depending on type and pathaphysiology of the aneurysm. For instance, Hampikian et al [94] designed a coil for the treatment of intracranial aneurysms which requires treatment with coil embolization due to the relatively narrow neck areas. The coil designed incorporated a trademark SMPU with T_g 33 °C. However, shape memory properties were inadequate. Metcalfe et al. [95] designed an endovascular foam using a trademark polyurethane-based foam. The foam showed no cytotoxicity or mutagenicity, and its porous structure enables cellular invasion and neointima formation. However,

the T_g of the foam was 60 °C. Baker et al [96] synthesized an SMP foam composed of poly(ε-caprolactone)-co-poly(ethylene glycol) (PCL-co-PEG). The foam showed various T_ms, between body temperatures to 80 °C. Although the foam had T_m close to body temperature, expansion was observed around 5 minutes. The methods that are effective in treating wide-necked aneurysms are not always a viable option for fusiform aneurysms due to the difficulties in defining aneurysm neck. Small et al [97] designed a stent-foam device for endovascular embolization of non-necked fusiform aneurysms. The SMP stent was obtained by dip coating stainless-steel pin with commercially available thermoplastic and laser-absorbing dyes. Due to the trademark dyes, final T_g of the stent was 55 °C. Same laser-absorbing dye is incorporated into the foam to enable light-absorption. Overall, the stent-foam design was not suitable to use within human body.

Clot removal devices are another type of medical devices. Due to the location of the clot imminent removal is required to negate or minimize effects (i.e., stroke). As the patient is already losing time while reaching hospitals, conventional methods in such crucial situations with limited time fail to make up for the time lost. Metzger et al. [98] designed SMP microactuators for stroke treatment. The devices were designed from trademark ester-based thermosetting polyurethanes that have different mechanical and thermal properties and had T_gs above body temperature. Similarly, Small et al. [99] designed a thrombectomy device utilizing trademark PU. The device was activated with a laser (803 nm) with light-absorbing dye. Computer simulation of the device in air condition showed that 93% of the light can reach the distal end. Although device deployment time was relatively fast (around 3 seconds), only 43% of the light was transmitted to the distal end of the device (tested in a blood environment) due to refractive index of blood. Additionally, another thrombectomy device is designed [100]. The device was a combination of SMPU which is synthesized from HDI, HPED, and TEA, and a commercial nitinol wire which is also used for heat delivery. T_g of the synthesized SMPU was found to be tailorable between 34 °C and 86 °C.

1.3 List of publications produced from the thesis

1. Shape Memory Polyurethane Synthesis by Using Glycerol as Chain Extender for Biomedical Applications, Serap Başkır, Alican Onur Cankaya, Emre Tekay, Berkay Erenay, Bora Garipcan, Özgür Kocatürk, "Polymer International", 2024.

1.4 Overview of thesis

This study aimed to synthesize an SMPU using Glycerol as chain extender with a glass transition temperature within a suitable temperature range for biomedical applications. The results showed that the triggering temperatures for the synthesized samples changes between 63.95 °C and 88.21 °C. Shape memory properties were investigated for the temperature range of 40 °C and 75 °C. Shape recovery times were found to be substantially with increasing temperature with 102 seconds at 40 °C and 1 second at 75 °C. Shape fixity and shape recovery rates for the same temperature ranges were 77.8 % & 85.6 % at 40 °C and 100 % & 100 % for 75 °C. Cytotoxicity assay indicate promising biocompatibility of the synthesized material for biomedical purposes. Overall, the synthesized polymers were found to be a potential candidate for biomedical applications such as stents, aneurysm filling, or occlusion devices.

2. SHAPE MEMORY POLYURETHANE SYNTHESIS BY USING GLYCEROL AS CHAIN EXTENDER FOR BIOMEDICAL APPLICATIONS

2.1 Introduction

Shape memory materials (SMMs) represent a sophisticated group of materials with the unique ability to modify their shape when subjected to specific external stimuli, such as water, heat, pH changes, light, and magnetic field [101],[102],[82]. SMMs are intricately characterized by their dual-shape capability, wherein they possess a permanent shape and a temporary shape [4],[103]. The temporary shape refers to an altered state of the material that is designed to be maintained temporarily under specific conditions until a triggering stimulus is applied. At this point, the material reverts or transitions to its permanent shape which is the original configuration. These unique behaviors of SMMs broaden their applicability in various fields including but not limited to biomedical engineering, robotics, and aerospace where materials with dynamic shape-changing capabilities are increasingly in demand [104],[105]..

These smart materials are categorized into shape-memory ceramics (SMCs), shape-memory alloys (SMAs), and shape-memory polymers (SMPs) [106]. SMAs are popular in many fields due to the advantages of corrosion and abrasion resistance as well as attractive mechanical attributes [104], and SMCs have the properties of higher strength, high operating temperatures, and excellent corrosion and oxidation resistances [107] that enabled these materials to be used in many fields [108],[109]. However, a significant limitation of these materials is their lack of biodegradability, which necessitates additional medical procedures for extraction or removal from the body post-application. In contrast, SMPs offer the distinct advantage of tunable biodegradability [81], a critical feature allowing for customization of degradation time to meet the specific design constraints of various medical devices. This ability to adjust the degradation rate effectively eliminates the need for secondary surgical interventions

to remove these materials. Furthermore, SMPs present additional advantages including [23] ease of processability, cost-effectiveness, lightweight nature, biocompatibility, programmability of shape recovery, and, notably, adjustable stiffness. By providing biocompatibility and varying degrees of flexibility or rigidity, SMPs minimize the risk of adverse reactions, making them the preferable candidates for biomedical applications [81],[25],[24],[110].

For the utilization of SMP in the biomedical field, Polyurethane (PU) emerges as a material of significant interest, distinguished by its versatile application in medical devices and its intrinsic composition of soft and hard segments [26],[8]. This duality in its molecular structure grants PU flexibility and rigidity with an exemplary balance, fitting for biomedical applications [27]. The molecular homogeneity inherent in PU's chain molecules ensures uniformity at a molecular scale, facilitating enhanced compatibility with biological systems [8]. Another notable advantage of PU-based SMPs is their extensive temperature range for effective shape recovery and through the adjustment of the soft/hard segment ratio the ability to design the triggering temperature which may be glass transition temperature (T_g) or melting temperature (T_m) [26],[8]. Additionally, PU exhibits remarkable high strain recoveries, an attribute critical in applications requiring durability and resilience. Overall, these properties make polyurethane a highly favored material in the synthesis of SMPs tailored for biomedical purposes [26],[8].

Several studies in the biomedical field, particularly in vascular applications, prioritize the synthesis and utilization of shape-memory polyurethanes (SMPU). For stents, self-deployment using the body temperature as the trigger stimulus is vastly researched [89],[90],[91],[86],[111]. This feature is studied to help to optimize the device profile as well as the surgical procedure time. Furthermore, in a similar context, potential removal options for the vascular stent are studied with focusing on the biodegradability of the SMPs [88] and the materials unique shape change characteristics [86]. Occlusion devices are another example where SMPs are incorporated into design to enhance treatment effectiveness. Earlier aneurysm filling device designs focused on utilizing the mechanical properties (e.g., adjustable stiffness) of SMPs to minimize rupture risk of the weak intracranial aneurysm walls [94],[95],[96]. Furthermore, en-

dothelization with the biodegradability of the SMPs to enhance treatment and healing is another aspect investigated in various occluding devices such as ductus arteriosus occlusion [112], and intracranial [113] and peripheral occlusion devices [114],[115].

This study aimed to synthesize an SMPU using Glycerol as chain extender with a glass transition temperature within a suitable temperature range for biomedical applications. For this, SMPU samples were synthesized using Hexamethylene diisocyanate (HDI), N,N,N',N'-Tetrakis (2-hydroxypropyl) ethylenediamine (HPED), and Glycerol (GLY). HDI and HPED were chosen due to aliphatic monomers having better biocompatibility over aromatic monomers [30] and resulting with better mechanical properties [57]. Glycerol was chosen as it enhances the polymer's flexibility, reduces thermal stability and glass transition temperature [116], and increases tensile strength & ductility while decreasing Young's modulus [117]. Thermomechanical and shape-memory properties of the synthesized SMPU samples were studied as a function of their compositions.

2.2 Materials and Methods

2.2.1 Materials

The monomers Hexamethylene diisocyanate (HDI), N,N,N',N' - Tetrakis (2 - hydroxypropyl) ethylenediamine (HPED), and Glycerol (GLY) were used as received (Sigma Aldrich, USA). The monomer combinations were given at Table 2.1. DMEM-F12 and FBS purchased from Biosera, France.

SMPU samples were synthesized using one-shot method. During the addition step, HPED and Glycerol were weighed in the same beaker and HDI was weighed with different beaker and then added to others. Synthesis of the samples were done in small batches (7-10 grams), and the stirring time (2.5-3 minutes) and stirring speed kept low in order to minimize polymerization & resultant bubble formations. Degassing was done in -0.9 bar vacuum for 5-10 minutes. To form the samples the mixtures were

Table 2.1
Monomer Ratios (moles) of the samples using HDI (Hexamethylene diisocyanate), HPED (N,N,N',N'-Tetrakis (2-hydroxypropyl) ethylenediamine), and GLY (Glycerol). A total of 5 different samples are synthesized using these three monomers with given mole ratios.

Sample	HDI	HPED	GLY
SMPU-GLY3%	1	0.208	0.0426
SMPU-GLY4%	1	0.449	0.0663
SMPU-GLY9%	1	0.180	0.120
SMPU-GLY11%	1	0.475	0.0334
SMPU-GLY17%	1	0.302	0.266

poured in custom-made silicone molds (dimensions 7.5 cm x 7.5 cm x 0.05 cm). Curing was done in a sealed oven preheated to 140 °C, and the specimens were cured for one hour, as it is illustrated in Figure 2.1. The samples were named as SMPU-GLY3%, SMPU-GLY4%, SMPU-GLY9%, SMPU-GLY11%, and SMPU-GLY17%, according to their percentage ratio of glycerol content.

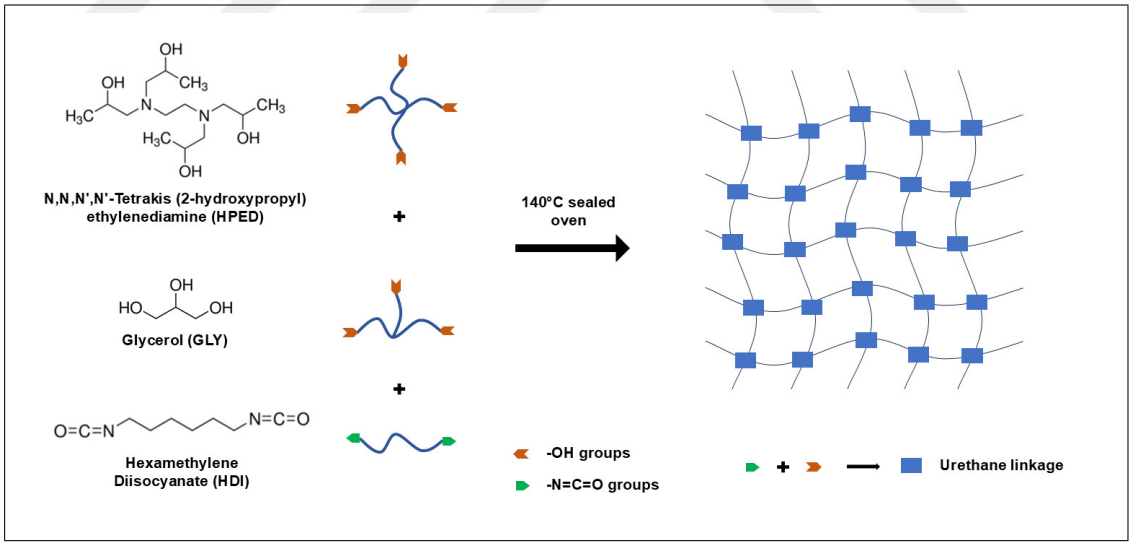


Figure 2.1 Schematic representation of the monomers used in the study and the polymer network of synthesized SMPU samples.

2.3 Characterization of the SMPU samples

2.3.1 Thermogravimetric Analysis

The thermal stability of the produced PUs was determined using a TGA-Q50 (TA Instruments, USA) device. The analysis was performed in a nitrogen atmosphere (temperature range 200 °C - 600 °C and heating rate 10°C / min).

2.3.2 Differential Scanning Calorimetry

DSC analyses were performed using a DSC-Q200 (TA Instruments, USA) device. The measurements were done in a nitrogen atmosphere (temperature range 0 °C - 100 °C and heating rate 10 °C / min).

2.3.3 Fourier Transform Infrared Spectroscopy

Fourier transform infrared (FTIR) spectra data were collected with ATR method with an FTIRSPRIT (Shimadzu, Japan). Scan rate 45 Hz, wavelength range 400-4000 nm. 10 scans for each sample were taken in intensity mode (resolution 4 $cm^{-}1$) with Happ-genzel function used for Apodization.

2.3.4 Dynamic Mechanical Analysis

The dynamic mechanical properties of the PUs were evaluated in tensile mode using a TMA-7100 (Hitachi, Japan) equipped with an electric cooler. The analyses were conducted on samples (dimensions 15 mm x 2 mm x 0.5 mm) at 0.1 Hz frequency (temperature range 30 °C to 135 °C and heating rate 3 °C / min).

2.3.5 Shape Memory Behaviour

Shape memory behaviour was evaluated using the following protocol: (1) Samples were deformed into a temporary shape under preheated water with various temperatures, then cooled in 5 °C water for shape fixing. Shape recovery is then achieved by placing the samples back into preheated water. Time taken for each sample to revert to its permanent shape was recorded with a video camera fixed above the heater. The initial shape, temporary shape, and recovered shape of the samples were also recorded exclusively. Shape recovery time was assessed with the camera recordings. For shape fixing ratio (R_f) and shape recovery ratio (R_s) the following equations were used [118]:

$$R_f(\%) = \frac{\theta}{\theta_1} \cdot 100 \tag{2.1}$$

$$R_s(\%) = \frac{\theta_2 - \theta}{\theta_2} \cdot 100 \tag{2.2}$$

Where R_f is the shape fixing ratio, R_s is the shape recovery ratio, and θ is the angle of deformation of the samples, θ_1 is the angle of the temporary shape and θ_2 is the angle of the permanent shape.

2.3.6 Cell Culture and MTT Cytotoxicity Assay

Potential leaching of unpolymerized HPED, HDI, and glycerol from samples and their consequential cytotoxic effects were assessed with MTT cytotoxicity assay. Sample extracts were prepared by following general guidelines given by ISO 10993-12:2021. Sample extraction ratio was selected as 6 cm^2 / mL, Dulbecco's Modified Eagle Medium F12 (DMEM-F12) complemented with 10 % Fetal Bovine Serum (FBS) and 1 % penicillin / streptomycin solution as extraction vehicle and extracted for 24 hours with aforementioned medium. Assessment of cytotoxicity through MTT assay

was conducted by following the general guidelines given by ISO 10993-5:2009. Briefly, mouse L929 fibroblasts (CCL-1, ATCC, Rockville, MD, USA) were seeded on 96-well plates with a seeding density of 1 x 104 cells / well and cultured with extraction vehicle (complete DMEM-F12) for 24 hours at 37 °C. Growth media from cells were aspirated and graded sample extracts (100 %, 75 %, 50 %, and 25 %) were added into wells. Extracts were diluted with complete DMEM-F12 medium from initial extract. Following an additional 24 hours of culture, 50 μL of sterile filtered 1 mg / mL MTT solution diluted with complete DMEM-F12 growth medium was added into each well and incubated for 2 hours at 37 °C. MTT solutions were then aspirated, and formazan crystals were dissolved with absolute isopropanol with gentle shaking in room temperature and absorbances were read at 570 nm. Incubation temperature and CO_2 levels for all cell culture experiments were 37 °C and 5 %, respectively. All measurements were done in six technical repeats. Statistical significance between experimental groups against negative control (vehicle) was tested with one-way ANOVA with a post-hoc Dunnett's multiple comparison test.

2.4 Results and Discussion

2.4.1 Thermogravimetric analysis

Thermogravimetric analysis (TGA) of the synthesized shape memory polymer samples was conducted to evaluate their thermal stability (Figure 2.2 and Table 2.2). Degradation onset SMPU-GLY4%, SMPU-GLY9%, SMPU-GLY3%, SMPU-GLY11%, SMPU-GLY17%, were at 236.34 °C, 228.03 °C, 234.12 °C, 216.16 °C, 249.10 °C, respectively. 90 % weight and 50 % weight of the samples were reached at 282.67 °C & 334.67 °C for SMPU-GLY4%, 282.68 °C & 391.79 °C for SMPU-GLY9%, 284.24 °C & 393.02 °C for SMPU-GLY3%, 295.79 °C & 410.80 °C for SMPU-GLY11%, and 279.38 °C & 381.12 °C for SMPU-GLY17%.

The thermogravimetric analysis (TGA) of the samples reveals the differences in their thermal stability. The degradation phase for all samples occurred between 216.16

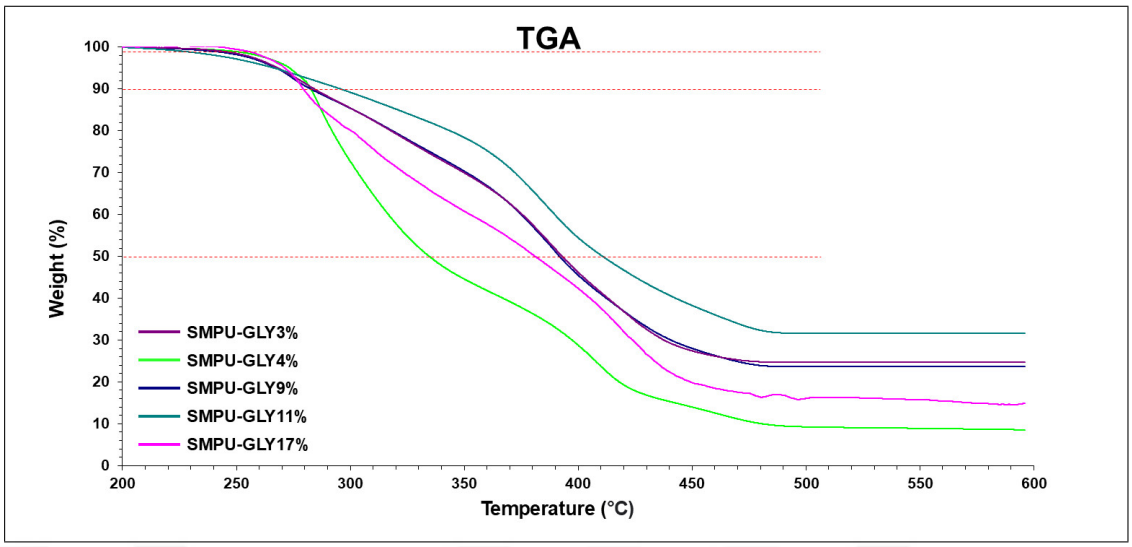


Figure 2.2 Thermogravimetric analysis (TGA) curves of the 5 SMPU samples. Onset of degradation and the temperatures at which 90% and 50% of the original weight retained are shown (red dashed lines).

°C and 410.80 °C, corresponding to the breakdown of the polymer backbone, indicated by the weight loss. The presence of urethane and urea linkages plays a critical role in this degradation behavior as increased crosslink density requires more energy to break down these bonds. This can be seen for SMPU-GLY17%, with higher ratio of HPED + GLY, showing a more extended degradation phase, suggesting that these linkages provide additional thermal stability[41].

Table 2.2
Thermal degradation profiles of the 5 SMPU samples from thermogravimetric analysis (TGA).

Sample	**Thermal deg. onset (°C)**	**90% weight remain at (°C)**	**50% weight remain at (°C)**	**Temperature at degradation peaks (°C)**	
				Peak 1	**Peak 2**
SMPU-GLY3%	234.12 °C	284.24 °C	393.02 °C	283.50 °C	391.60 °C
SMPU-GLY4%	236.34 °C	282.67 °C	334.67 °C	292.50 °C	413.00 °C
SMPU-GLY9%	228.03 °C	282.68 °C	391.79 °C	279.60 °C	391.30 °C
SMPU-GLY11%	216.16 °C	295.79 °C	410.80 °C	315.70 °C	391.70 °C
SMPU-GLY17%	249.10 °C	279.38 °C	381.12 °C	284.00 °C	421.80 °C

2.4.2 Differential Scanning Calorimetry

The Differential Scanning Calorimetry (DSC) analysis was conducted on the synthesized shape memory polymer samples to examine their thermal properties, specifically focusing on glass transition temperatures (T_g) (Figure 2.3 and Table 2.3). The T_g of the samples were 87.5 °C, 63.95 °C, 85.75 °C, 88.21 °C, and 72.45 °C, for SMPU-GLY4%, SMPU-GLY9%, SMPU-GLY3%, SMPU-GLY11%, SMPU-GLY17%, respectively.

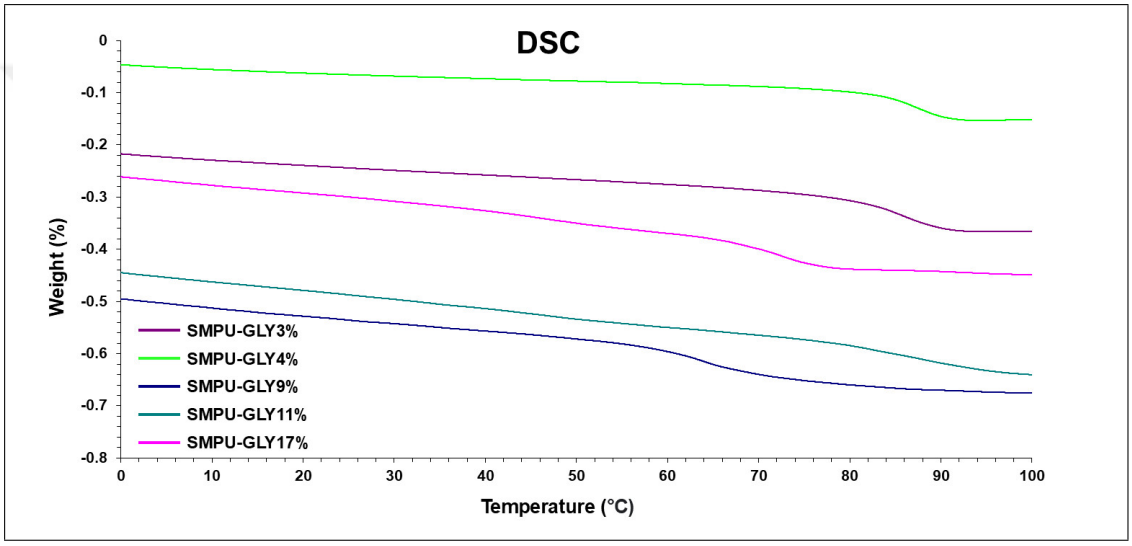


Figure 2.3 Differential Scanning Calorimetry (DSC) thermograms of the 5 SMPU samples, used for determination of T_g.

The Differential Scanning Calorimetry (DSC) curves revealed distinct differences in T_g among the samples. HDI provides rigid segments, while HPED contributes to flexible segments, balancing the overall polymer structure and enhancing thermal stability. Increased HPED content was shown to increase thermal transition temperature [30],[32]. This is apparent in our results as SMPU-GLY11% had the highest T_g with highest HPED content and SMPU-GLY9% had the lowest T_g with lowest HPED content. The higher crosslink density due to the high functionality of HPED resulted in an increase of T_g. Additionally, the methyl group introduced by the secondary OH group of HPED [30] causing steric hindrance can increase T_g. However, SMPU-GLY17% had a lower T_g than SMPU-GLY3% although SMPU-GLY17%'s HPED content is higher. This might be because of the increased GLY content which introduces hydroxyl groups

that form hydrogen bonds, disrupting the polymer network's rigidity and slightly altering the glass transition temperature [116]. Additionally, the -OH / -NCO ratio may potentially have an influence on this matter. The lower -OH / -NCO of SMPU-GLY3% could lead to side reactions and the formation of more urea bonds that would increase the overall cross-linking density and, consecutively result in a higher Tg compared to the SMPU-GLY17%. Similarly, SMPU-GLY9% might have relatively more urea bonds due to its low -OH / -NCO ratio. However, in the case of SMPU-GLY9%, the overall crosslink density might still be lower due to glycerol's geometry does not favoring tight crosslinking. Hence, SMPU-GLY9% had the lowest T_g.

Table 2.3
Glass transition Temperatures (T_g) of the 5 SMPU samples from differential scanning calorimetry (DSC) thermograms.

Sample	T_g **(DSC) (°C)**
SMPU-GLY3%	85.75 °C
SMPU-GLY4%	87.50 °C
SMPU-GLY9%	63.95 °C
SMPU-GLY11%	88.21 °C
SMPU-GLY17%	72.45 °C

2.4.3 Fourier Transform Infrared Spectroscopy

The FTIR spectra of the synthesized shape memory polymer samples were analyzed to identify the chemical structure and functional groups present (Figure 2.4).

Characteristic absorption peaks are shown in Figure 2.4: N-H stretching peak at $\sim 3330\ cm^{-1}$ observed in all samples, which is characteristic of the hydrogen-bonded N-H groups within the urethane linkages. The urethane linkage peak at $\sim 1695\ cm^{-1}$ suggests the successful formation of the urethane bond from the reaction of the isocyanate group of HDI and the hydroxyl groups of HPED and GLY. Peak $\sim 1650\ cm^{-1}$ could be attributed to urea linkages, which is likely the result of the reaction of excess isocyanate groups with water that can form during the synthesis or be present as mois-

ture. The C-H bending vibration around 1460 cm^{-1} indicates the existence of aliphatic CH_2 groups from HDI and possibly CH_3 groups from GLY. A peak at $\sim$ 1300 cm^{-1} aligns with the C-N stretching vibrations, suggesting successful incorporation of HDI. Overall, the FTIR findings confirm the formation of polyurethane.

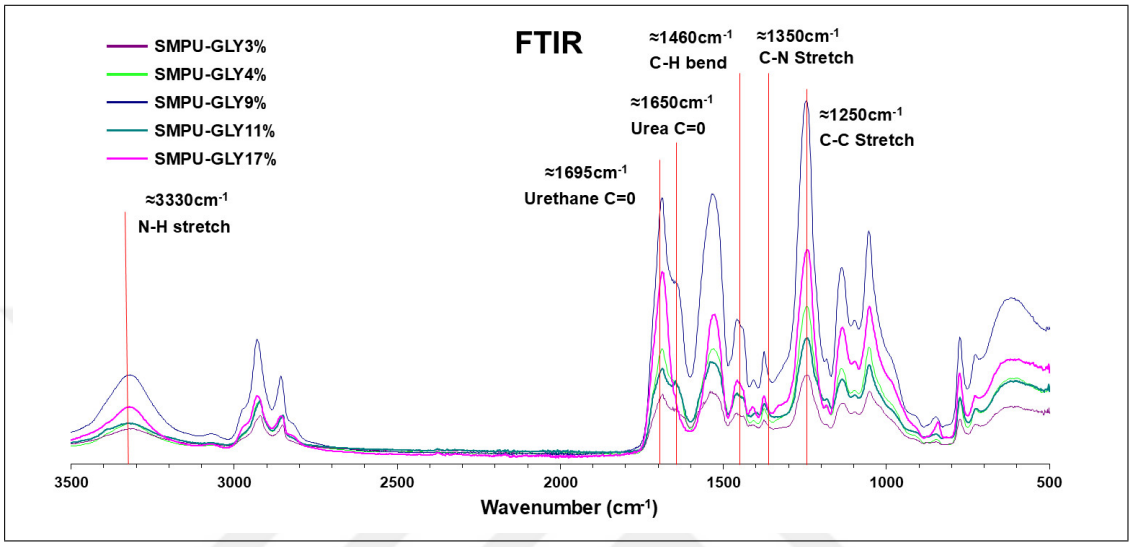


Figure 2.4 Fourier Transform Infrared (FTIR) spectra of the 5 SMPU samples synthesized using different ratios of HDI, HPED, and GLY monomers. Wavelengths of the bonds related to the expected polymer network are shown (red lines).

Absorption band peaks around 1650 cm^{-1} ($C = O$ bond), 1695 cm^{-1} ($C = O$), and 3330 cm^{-1} ($N - H$ stretch), correspond to, $C = O$ from urea, $C = O$ from urethane, and $N - H$ stretch from the amine functional groups between the urethane & urea linkages, respectively. These characteristic absorption peaks confirm the successful synthesis and formation of the desired polymer linkages. The variations in peak intensities among the different samples reflect differences in their monomer compositions, affecting their crosslinking density and, consequently, their physical, mechanical, and thermal properties. Samples with higher HPED and GLY content exhibit sharper peak intensity profiles, which can influence their physical and mechanical properties [116],[119]. At 1695 cm^{-1} SMPU-GLY4%, with higher HPED & GLY content, showed the most intense absorption peak with 0.06, suggesting a higher concentration of urethane linkages, contributing to its mechanical properties. In contrast, SMPU-GLY9%, with lower HPED & GLY content, had the least intense absorption peak with 0.004, has a lower crosslink density which depresses its glass transition temperature closer to body temperature. Moreover, the $C = O$ peak shift from 1710 $cm^{-}1$ - 1725 cm^{-1} that

previously reported [120],[121] to be around 1695 cm^{-1}, implicates a structure with stronger hydrogen bonds. Furthermore, presence of $C-H$ bending, $C-N$ stretching, and $C-C$ stretching indicates the presence of stable hydrocarbon chains and further corroborates the successful synthesis of the polymer matrix. These functional groups are integral to maintaining the polymer's structural framework and enhancing its mechanical properties. Overall, the FTIR spectra confirms the chemical composition of the synthesized SMPU, and the identified functional groups are consistent with the intended polymer.

2.4.4 Dynamic Mechanical Analysis

The Dynamic Mechanical Analysis (DMA) was performed on synthesized shape memory polyurethane samples to evaluate their mechanical properties and thermal transitions. The DMA curves show the loss factor (tan δ) and the storage modulus (E') as functions of temperature ((Figure 2.5 and Table 2.4)). The tan δ peaks for the samples were 78.78 °C for SMPU-GLY4%, 65.52 °C for SMPU-GLY9%, 81.66 °C for SMPU-GLY3%, 86.66 °C for SMPU-GLY11%, and 72.81 °C for SMPU-GLY17%. The storage moduli for the sample were 4.69 x 107 MPa, 2.99 x 107 MPa, 1.62 x 107 MPa, 2.73 x 107 MPa, 7.31 x 107 MPa for SMPU-GLY4%, SMPU-GLY9%, SMPU-GLY3%, SMPU-GLY11%, and SMPU-GLY17%, respectively.

DMA curves reveal distinct differences in tan δ and storage modulus (E') among the samples. Similarly, here, the highest and lowest T_g indicated by the tan δ peaks were found to be 86.66 °C and 65.52 °C for SMPU-GLY11% and SMPU-GLY9%, respectively. As discussed before, this difference is attributed to the decreasing HPED content. The differences in T_g values of DSC and DMA originate from the different testing parameters such as heating rate for DSC or testing frequency of DMA [122]. Furthermore, the inherent recordings of DSC and DMA differ [122],[123]: (1) DSC measures T_g based on changes in heat capacity as the polymer transitions from a glassy to a rubbery state by providing a controlled heating rate in an inert atmosphere, and (2) DMA measures T_g based on changes in mechanical properties, reflecting material's mechanical response

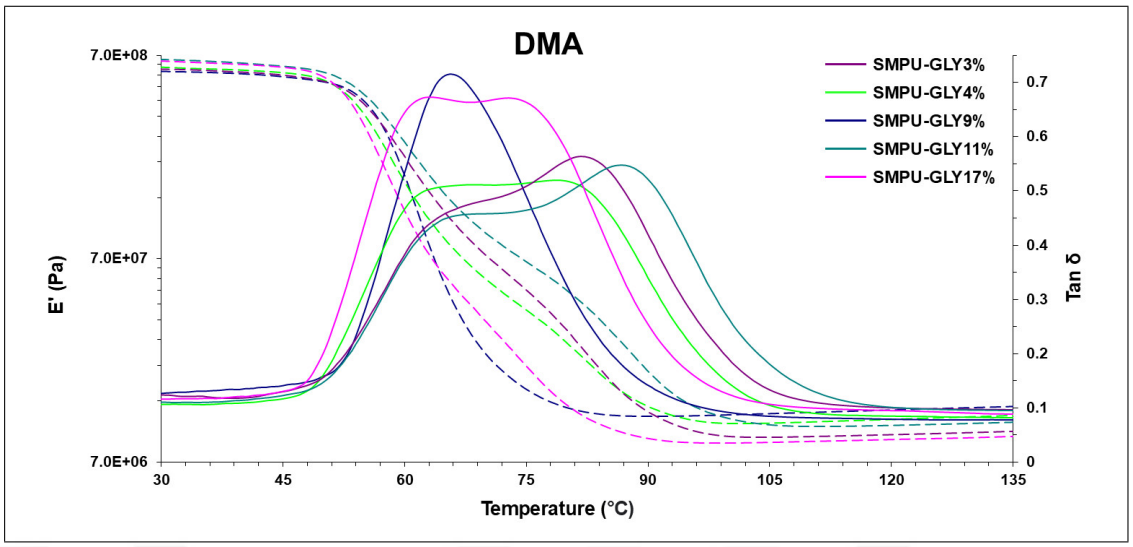


Figure 2.5 Dynamic Mechanical Analysis (DMA) of Shape Memory Polyurethane (SMPU) samples showing the temperature-dependent variations in storage modulus (E') and damping factor (tan δ) of the 5 SMPU samples (dashed lines and constant lines, respectively).

to temperature changes under dynamic mechanical force.

Table 2.4
Glass transition Temperatures (T_g) and storage modulus (E') of the 5 SMPU samples from Dynamic Mechanical Analysis (DMA).

Sample	**T_g (DMA) (°C)**	**E' (Storage Modulus) (MPa)**
SMPU-GLY3%	81.66 °C	16.2
SMPU-GLY4%	78.78 °C	46.9
SMPU-GLY9%	65.52 °C	29.9
SMPU-GLY11%	86.66 °C	27.3
SMPU-GLY17%	72.81 °C	73.1

Additionally, DMA's sensitivity to the mechanical response of the polymer network, including crosslinking and chain mobility, allows it to detect subtle changes in viscoelastic behavior that may not be as apparent in DSC measurements. Hence, similar differences are seen in literature between two testing procedures [30],[123],[124],[125], [126].

The storage moduli of the samples in the glassy region (at 25 °C) provide in-

formation about their elastic properties both in their original and temporary shapes (Table 2.4). The storage moduli for the samples at 25 °C were measured as 598 MPa, 666 MPa, 591 MPa, 682 MPa, 621 MPa for SMPU-GLY3%, SMPU-GLY4%, SMPU-GLY9%, SMPU-GLY11%, and SMPU-GLY17%, respectively. The storage modulus values increased proportionally with the amount of HPED in the samples with the highest value was obtained for SMPU-GLY11%, while the lowest value was recorded for SMPU-GLY9%. This can be attributed to the higher crosslink density. As the crosslink density increases, the restriction of molecular movements and the improved interconnectivity of the hard segment may enhance the elastic properties [127]. The storage moduli of all samples exhibited substantial reductions in the T_g region due to the transition from the glassy to the rubbery phase. While SMPU-GLY9% exhibited a single-step modulus reduction within a relatively narrow temperature range, the other samples transitioned to the rubbery phase in a two-step process over a significantly broader temperature range. A similar behavior is also observed in the tan δ graphs, where two peak maxima or broad peaks are found for all samples except SMPU-GLY9%. These broad peaks might be a result of non-homogeneous crosslink densities, high polydispersity, due to the varying degrees of phase mixing between the hard and soft segments, as well as the influence of morphology on the mechanical properties [127].

Table 2.5
Storage modulus (E') and tan δ of the 5 SMPU at 25 °C.

Sample	**E' (Storage Modulus) (MPa)**	**tan δ**
SMPU-GLY3%	598	0.13346
SMPU-GLY4%	666	0.12724
SMPU-GLY9%	591	0.10695
SMPU-GLY11%	682	0.11240
SMPU-GLY17%	621	0.11661

After the glass transition temperature, the storage modulus values of the samples decrease by approximately two orders of magnitude. However, in the rubbery plateau, the samples maintain an elastic character sufficient to support thermo-responsive shape

recovery. The damping parameter values (tan δ) of SMPU-GLY3%, SMPU-GLY4%, SMPU-GLY9%, SMPU-GLY11%, and SMPU-GLY17% at 25 °C were measured as 0.133, 0.127, 0.107, 0.112, and 0.117, respectively. The damping parameters in the glassy region (25 °C) did not show a clear trend based on composition.

2.4.5 Shape Memory Properties

The shape memory properties of the samples were evaluated through a series of experiments conducted in water at varying temperatures (Figure 2.6). Figure 2.6A shows the shape recovery time for the five samples at 60 °C. SMPU-GLY9% exhibited the shortest recovery time, followed by SMPU-GLY4%, SMPU-GLY3%, SMPU-GLY17%, and SMPU-GLY11%. Figure 2.6B shows the shape recovery time of SMPU-GLY9% temperatures ranging from 40 °C to 75 °C. Recovery time decreased substantially with increasing temperature, with highest recovery time being ∼102 seconds at 40 °C and lowest recovery time being ∼1 second at 75 °C. Figure 2.6C displays the shape fixity and shape recovery ratios for SMPU-GLY9% at different temperatures. At 40 °C, shape fixity was 77.8% and shape recovery was 85.6% for SMPU-GLY9%. At 45 °C, shape fixity was 100% and shape recovery was 91.1% for SMPU-GLY9%. For the remaining temperatures, SMPU-GLY9% showed 100% shape fixity & shape recovery.

Figure 2.7 illustrates the permanent, temporary, and recovered shapes for all samples at 60 °C (Figure 2.7A) and SMPU-GLY9% at varying temperatures (Figure 2.7B). All samples showed 100% shape fixity & shape recovery at 60°C. For 40 °C and 45 °C, SMPU-GLY9% showed 77.8% & 100% shape fixity and 85.6% and 91.1% shape recovery, respectively. For temperatures 50 °C -75 °C, both shape fixity and shape recovery were 100%.

All samples showed excellent shape fixity and shape recovery at 60 °C within reasonable recovery times. However, the shortest recovery time 60 °C was for SMPU-GLY9% with 21 seconds, making it a suitable candidate for biomedical applications requiring quick response times. This was due to its lower HPED and GLY content which

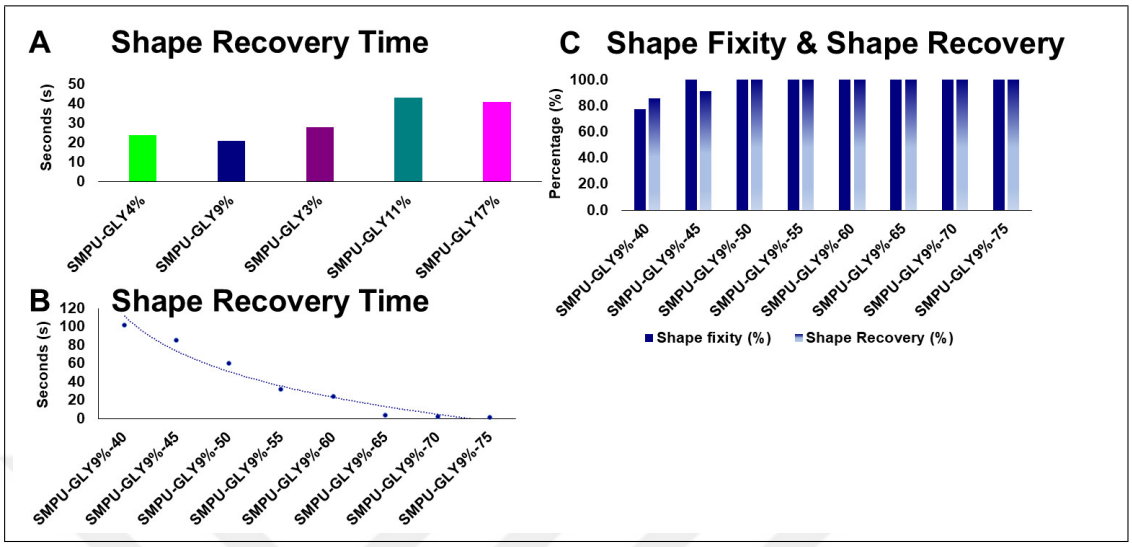


Figure 2.6 Shape memory properties of the 5 SMPU samples. (A) Shape recovery times of samples 1 to 5 at 60 °C and (B) shape recovery times of SMPU-GLY9% at varying temperatures (40 °C - 75 °C). (C) Shape Fixity and shape recovery ratios of SMPU-GLY9% at varying temperatures (40 °C - 75 °C).

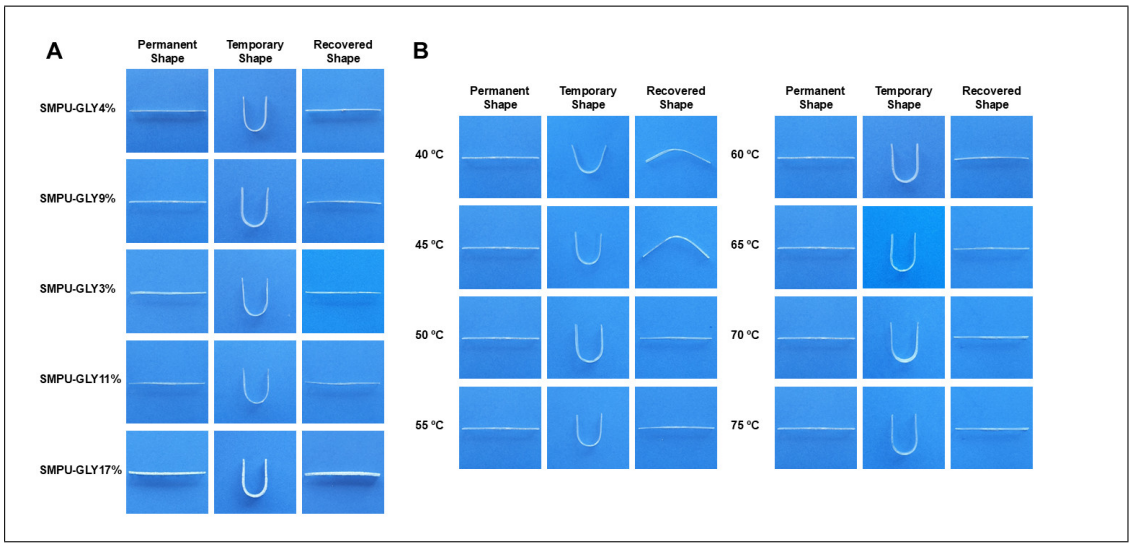


Figure 2.7 Permanent, temporary, and recovered shapes for (A) SMPU-GLY4%, SMPU-GLY9%, SMPU-GLY3%, SMPU-GLY11%, and SMPU-GLY17% at 60 °C and (B) SMPU-GLY9% at varying temperatures (40 °C -75 °C).

resulted in lower Tg and its rapid recovery. Additional shape recovery properties were recorded at temperatures ranging from 40 °C to 75 °C to explore the potential of SMPU-GLY9%. Good shape fixity and shape recovery observed throughout the temperatures studied, and the recovery time decreased with increasing temperature, indicating that higher temperatures facilitate faster shape recovery. This trend of SMPU-GLY9% recovery time highlights its potential for applications where quick shape recovery is critical.

2.4.6 Cell culture and MTT cytotoxicity assay

Following the promising shape recovery rate and thermal stability of SMPU-GLY9%, it was selected as model candidate for cytotoxicity testing. Adherent L929 cell viabilities were unchanged and graded extract treatments didn't result in a statistically significant difference in comparison with the control (Figure 2.8). An extract is regarded to be cytotoxic when its measured viability results below 70% that of the control group [128]. This observation shows extremely promising biocompatibility of SMPU-GLY9%, as even the highest concentration of extract treated cells resulted in the statistically similar cellular viabilities compared to the control group in terms of leachate cytotoxicity. However, further investigations of behavior of cells within direct contact to the material surfaces are required to have a comprehensive understanding before in-vivo studies.

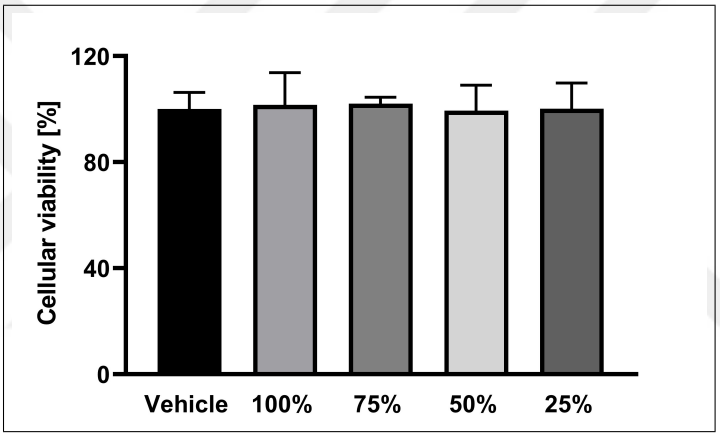


Figure 2.8 Cellular viability of L929 mouse fibroblasts after 24 hours of culture with extract treatments, assessed with an MTT assay. Percent values are graded dilutions of SMPU-GLY9% extract, diluted with complete DMEM-F12. Absorbances at 570 nm of each experimental group were normalized to vehicle control and presented as such. No statistical significance was observed between groups treated with graded extracts against vehicle control.

3. DISCUSSION

This study aimed to synthesize an SMPU using Glycerol as chain extender with a glass transition temperature within a suitable temperature range for biomedical applications. For this purpose, a series of samples were synthesized and their thermal properties, mechanical properties, biocompatibility, and shape memory properties were assessed.

Previously, water absorption was shown to affect thermal transition temperature [129],[130]. This is most likely due to the plasticization effect [131], where the water acts as plasticizer and weakening the hydrogen bonding between $N-H$ and $C=O$ groups. Two important parameters to control this effect would be the conditioning time of the material and the porous structure of the material. Parameters like humidity level, temperature, and exposure time is also shown to control this effect [132], with longer exposure time resulting with lower T_g values. Furthermore, storage conditions (e.g., humidity, temperature) may also affect the material shape memory properties [34],[70] and affect device performance [40]. Although such pre-conditioning was not performed, T_gs of the samples studied here are close to the general range for safe tissue-material interaction (37 °C-41 °C [133],[134],[135],[136]) and suitable for short-term interaction ($\sim$3 seconds around 65 °C [134]). Hence, a substantial shift in the T_g and improving suitability for biomedical applications can be achieved with proper pre-conditioning. Overall, consideration of such pre-conditioning is vital for designing the T_g of the material within a range that is applicable for biomedical applications and would require extensive and exhaustive research that should be done separately.

A novel property of the medical devices designed with shape memory polymers is the ease of device deployment where the trigger stimulus of the SMP eliminates the need of additional mechanisms [137]. As such, the SMPU studied here can be programmed to utilize body temperature as its stimuli in order to reduce the device profile. The material synthesized here can potentially be used in the design of self-

deployment stents. This is further supported by the lightweight and adjustable nature of the polymer material that enhances the compatibility with the tissue and minimizes the risk of tissue damage in deployment. Moreover, shape memory properties indicate good shape recovery and fast deployment around the body temperature. This is especially pronounced for SMPU-GLY9%, where the material shows deployment around 3 seconds, within the acceptable range without tissue damage [134]. These combined properties indicate their potential to be used in the design of aneurysm filling devices or occlude devices where fast deployment is required to minimize risk of migration [138].

Initial evaluation of the SMPU demonstrated promising biocompatibility, as indicated by the MTT assay results. The viability of L929 mouse fibroblasts remained above the critical 70% threshold across all graded extract concentrations, showing no statistically significant deviation from the vehicle control. This outcome suggests that the material does not elicit cytotoxic responses under the tested conditions, underscoring its potential suitability for biomedical applications. However, while these in vitro findings are encouraging, they emphasize the necessity for further investigations. For biomaterials intended for medical applications, ensuring comprehensive biocompatibility is essential, and this involves rigorous testing in line with ISO 10993 standards [139]. These tests depend on the contact type, the type of tissue the material is in contact with and contact duration. The material studied here would be considered to be in contact with blood, and the duration would be dependent on the medical device type (e.g., clot removal, aneurysm filling, occlusion, stent). Short-term exposure typically necessitates the basic characteristic tests (i.e., cytotoxicity, sensitization, and irritation) to assess to verify initial biocompatibility. Extensive tests (such as systemic toxicity and subacute toxicity) are needed to ensure safety over days or weeks and for materials requiring long-term exposure, particularly for implantable devices or materials contacting tissue or blood for more than 30 days, requires thorough (e.g., chronic toxicity, genotoxicity and carcinogenicity, hemocompatibility and implantation studies) evaluations. Additionally, degradation product analysis becomes crucial to understand how the material breaks down in vivo and the potential effects of these byproducts. Such analysis is required to fully establish the safety profile and suitability of the biomaterial for clinical applications. While aliphatic monomers, known to pose

a lower cancer risk compared to aromatic monomers, are utilized in these materials, there is still a possibility that potentially harmful degradation products could form. Literature indicates that although such degradation products can be identified, the levels of exposure are typically well within safe limits and significantly below regulatory thresholds [42]. Nonetheless, comprehensive and detailed studies are essential as the material development advances, ensuring that any degradation byproducts are thoroughly assessed. This further analysis would be crucial to verify the long-term safety and biocompatibility of these materials, solidifying their viability for use in medical devices.

The aim of this study was to synthesize an SMPU using Glycerol as chain extender with a glass transition temperature within a suitable temperature range for biomedical applications. Among the synthesized samples, SMPU-GLY9% was found to be the most promising candidate. Noting that additional work is required on adjustment of the T_g, characterization of the SMPUs indicated that GLY can be used as chain extender to improve the suitability of the SMPU for biomedical devices by enhancing its mechanical properties and decreasing its T_g. Combining with its promising biocompatibility, the SMPU synthesized here has the potential for designing biomedical devices such as stents, aneurysm filling devices, or occlusion devices that can be explored with further studies.

REFERENCES

1. Hager, M. D., S. Bode, C. Weber, and U. S. Schubert, "Shape memory polymers: Past, present and future developments," *Progress in Polymer Science*, Vol. 49-50, pp. 3–33, Oct. 2015.

2. Dayyoub, T., A. V. Maksimkin, O. V. Filippova, V. V. Tcherdyntsev, and D. V. Telyshev, "Shape Memory Polymers as Smart Materials: A Review," *Polymers*, Vol. 14, p. 3511, Aug. 2022.

3. Panahi-Sarmad, M., M. Abrisham, M. Noroozi, A. Amirkiai, P. Dehghan, V. Goodarzi, and B. Zahiri, "Deep focusing on the role of microstructures in shape memory properties of polymer composites: A critical review," *European Polymer Journal*, Vol. 117, pp. 280–303, Aug. 2019.

4. Hu, J., Y. Zhu, H. Huang, and J. Lu, "Recent advances in shape–memory polymers: Structure, mechanism, functionality, modeling and applications," *Progress in Polymer Science*, Vol. 37, pp. 1720–1763, Dec. 2012.

5. Zhao, Q., H. J. Qi, and T. Xie, "Recent progress in shape memory polymer: New behavior, enabling materials, and mechanistic understanding," *Progress in Polymer Science*, Vol. 49-50, pp. 79–120, Oct. 2015.

6. Mu, T., L. Liu, X. Lan, Y. Liu, and J. Leng, "Shape memory polymers for composites," *Composites Science and Technology*, Vol. 160, pp. 169–198, May 2018.

7. Li, G., and A. Wang, "Cold, warm, and hot programming of shape memory polymers," *Journal of Polymer Science Part B: Polymer Physics*, Vol. 54, pp. 1319–1339, July 2016.

8. Thakur, S., and J. Hu, "Polyurethane: A Shape Memory Polymer (SMP)," in *Aspects of Polyurethanes* (Yilmaz, F., ed.), InTech, Sept. 2017.

9. Liu, C., H. Qin, and P. T. Mather, "Review of progress in shape-memory polymers," *Journal of Materials Chemistry*, Vol. 17, no. 16, p. 1543, 2007.

10. Ratna, D., and J. Karger-Kocsis, "Recent advances in shape memory polymers and composites: a review," *Journal of Materials Science*, Vol. 43, pp. 254–269, Jan. 2008.

11. Leng, J., X. Lan, Y. Liu, and S. Du, "Shape-memory polymers and their composites: Stimulus methods and applications," *Progress in Materials Science*, Vol. 56, pp. 1077–1135, Sept. 2011.

12. Bhanushali, H., S. Amrutkar, S. Mestry, and S. T. Mhaske, "Shape memory polymer nanocomposite: a review on structure–property relationship," *Polymer Bulletin*, Vol. 79, pp. 3437–3493, June 2022.

13. Wang, K., S. Strandman, and X. X. Zhu, "A mini review: Shape memory polymers for biomedical applications," *Frontiers of Chemical Science and Engineering*, Vol. 11, pp. 143–153, June 2017.

14. Abrisham, M., M. Noroozi, M. Panahi-Sarmad, M. Arjmand, V. Goodarzi, Y. Shakeri, H. Golbaten-Mofrad, P. Dehghan, A. Seyfi Sahzabi, M. Sadri, and L. Uzun, "The role of polycaprolactone-triol (PCL-T) in biomedical applications: A state-of-the-art review," *European Polymer Journal*, Vol. 131, p. 109701, May 2020.

15. Arzberger, S. C., M. L. Tupper, M. S. Lake, R. Barrett, K. Mallick, C. Hazelton, W. Francis, P. N. Keller, D. Campbell, S. Feucht, D. Codell, J. Wintergerst, L. Adams, J. Mallioux, R. Denis, K. White, M. Long, N. A. Munshi, and K. Gall, "Elastic memory composites (EMC) for deployable industrial and commercial applications," (San Diego, CA), p. 35, May 2005.

16. Chen, T., O. R. Bilal, R. Lang, C. Daraio, and K. Shea, "Autonomous Deployment of a Solar Panel Using Elastic Origami and Distributed Shape-Memory-Polymer Actuators," *Physical Review Applied*, Vol. 11, p. 064069, June 2019.

17. Liu, Y., H. Du, L. Liu, and J. Leng, "Shape memory polymers and their composites in aerospace applications: a review," *Smart Materials and Structures*, Vol. 23, p. 023001, Feb. 2014.

18. Huang, X., M. Ford, Z. J. Patterson, M. Zarepoor, C. Pan, and C. Majidi, "Shape memory materials for electrically-powered soft machines," *Journal of Materials Chemistry B*, Vol. 8, no. 21, pp. 4539–4551, 2020.

19. Scalet, G., "Two-Way and Multiple-Way Shape Memory Polymers for Soft Robotics: An Overview," *Actuators*, Vol. 9, p. 10, Feb. 2020.

20. Stoychev, G., A. Kirillova, and L. Ionov, "Light-Responsive Shape-Changing Polymers," *Advanced Optical Materials*, Vol. 7, p. 1900067, Aug. 2019.

21. Xia, Y., Y. He, F. Zhang, Y. Liu, and J. Leng, "A Review of Shape Memory Polymers and Composites: Mechanisms, Materials, and Applications," *Advanced Materials*, Vol. 33, p. 2000713, Feb. 2021.

22. Sun, L., W. Huang, Z. Ding, Y. Zhao, C. Wang, H. Purnawali, and C. Tang, "Stimulus-responsive shape memory materials: A review," *Materials & Design*, Vol. 33, pp. 577–640, Jan. 2012.

23. Zhao, W., L. Liu, F. Zhang, J. Leng, and Y. Liu, "Shape memory polymers and their composites in biomedical applications," *Materials Science and Engineering: C*, Vol. 97, pp. 864–883, Apr. 2019.

24. Chien, Y.-c., W.-T. Chuang, U.-S. Jeng, and S.-h. Hsu, "Preparation, Characterization, and Mechanism for Biodegradable and Biocompatible Polyurethane Shape Memory Elastomers," *ACS Applied Materials & Interfaces*, Vol. 9, pp. 5419–5429, Feb. 2017.

25. Serrano, M. C., and G. A. Ameer, "Recent Insights Into the Biomedical Applications of Shape-memory Polymers," *Macromolecular Bioscience*, Vol. 12, pp. 1156–1171, Sept. 2012.

26. Fu, Y., W. Huang, J. Luo, and H. Lu, "Polyurethane shape-memory polymers for biomedical applications," in *Shape Memory Polymers for Biomedical Applications*, pp. 167–195, Elsevier, 2015.

27. Touchet, T., and E. Cosgriff-Hernandez, "Hierarchal structure–property relationships of segmented polyurethanes," in *Advances in Polyurethane Biomaterials*, pp. 3–22, Elsevier, 2016.

28. Cui, M., Z. Chai, Y. Lu, J. Zhu, and J. Chen, "Developments of polyurethane in biomedical applications: A review," *Resources Chemicals and Materials*, Vol. 2, pp. 262–276, Dec. 2023.

29. Menon, A. V., G. Madras, and S. Bose, "The journey of self-healing and shape memory polyurethanes from bench to translational research," *Polymer Chemistry*, Vol. 10, no. 32, pp. 4370–4388, 2019.

30. Wilson, T. S., J. P. Bearinger, J. L. Herberg, J. E. Marion, W. J. Wright, C. L. Evans, and D. J. Maitland, "Shape memory polymers based on uniform aliphatic urethane networks," *Journal of Applied Polymer Science*, Vol. 106, pp. 540–551, Oct. 2007.

31. Rodriguez, J. N., Y.-J. Yu, M. W. Miller, T. S. Wilson, J. Hartman, F. J. Clubb, B. Gentry, and D. J. Maitland, "Opacification of Shape Memory Polymer Foam Designed for Treatment of Intracranial Aneurysms," *Annals of Biomedical Engineering*, Vol. 40, pp. 883–897, Apr. 2012.

32. Singhal, P., J. N. Rodriguez, W. Small, S. Eagleston, J. Van de Water, D. J. Maitland, and T. S. Wilson, "Ultra low density and highly crosslinked biocompatible shape memory polyurethane foams," *Journal of Polymer Science Part B: Polymer Physics*, Vol. 50, pp. 724–737, May 2012.

33. Rodriguez, J. N., F. J. Clubb, T. S. Wilson, M. W. Miller, T. W. Fossum, J. Hartman, E. Tuzun, P. Singhal, and D. J. Maitland, "*In vivo* response to an implanted shape memory polyurethane foam in a porcine aneurysm model: Implantation of Shape Memory Polyurethane Foam," *Journal of Biomedical Materials Research Part A*, Vol. 102, pp. 1231–1242, May 2014.

34. Singhal, P., W. Small, E. Cosgriff-Hernandez, D. J. Maitland, and T. S. Wilson, "Low density biodegradable shape memory polyurethane foams for embolic biomedical applications," *Acta Biomaterialia*, Vol. 10, pp. 67–76, Jan. 2014.

35. Rodriguez, J. N., M. W. Miller, A. Boyle, J. Horn, C.-K. Yang, T. S. Wilson, J. M. Ortega, W. Small, L. Nash, H. Skoog, and D. J. Maitland, "Reticulation of low density shape memory polymer foam with an in vivo demonstration of vascular occlusion," *Journal of the Mechanical Behavior of Biomedical Materials*, Vol. 40, pp. 102–114, Dec. 2014.

36. Wang, X., Y. Li, J. Wei, and K. De Groot, "Development of biomimetic nanohydroxyapatite/poly(hexamethylene adipamide) composites," *Biomaterials*, Vol. 23, pp. 4787–4791, Dec. 2002.

37. Wang, J., R. Kunkel, J. Luo, Y. Li, H. Liu, B. N. Bohnstedt, Y. Liu, and C.-H. Lee, "Shape Memory Polyurethane with Porous Architectures for Potential Applications in Intracranial Aneurysm Treatment," *Polymers*, Vol. 11, p. 631, Apr. 2019.

38. Vakil, A. U., N. M. Petryk, E. Shepherd, H. T. Beaman, P. S. Ganesh, K. S. Dong, and M. B. B. Monroe, "Shape Memory Polymer Foams with Tunable Degradation Profiles," *ACS Applied Bio Materials*, Vol. 4, pp. 6769–6779, Sept. 2021.

39. Christmas, N., A. U. Vakil, C. J. Hatch, S. Dong, D. Fikhman, H. T. Beaman, and M. B. B. Monroe, "Characterization of shape memory polymer foam hemostats in in vitro hemorrhagic wound models," *Journal of Biomedical Materials Research Part B: Applied Biomaterials*, Vol. 109, pp. 681–692, May 2021.

40. Vakil, A. U., N. M. Petryk, C. Du, B. Howes, D. Stinfort, S. Serinelli, L. Gitto, M. Ramezani, H. T. Beaman, and M. B. B. Monroe, "In vitro and in vivo degradation correlations for polyurethane foams with tunable degradation rates," *Journal of Biomedical Materials Research Part A*, Vol. 111, pp. 580–595, May 2023.

41. Kunkel, R., D. Laurence, J. Wang, D. Robinson, J. Scherrer, Y. Wu, B. Bohnstedt, A. Chien, Y. Liu, and C.-H. Lee, "Synthesis and characterization of bio-compatible shape memory polymers with potential applications to endovascular embolization of intracranial aneurysms," *Journal of the Mechanical Behavior of Biomedical Materials*, Vol. 88, pp. 422–430, Dec. 2018.

42. Weems, A. C., K. T. Wacker, J. K. Carrow, A. J. Boyle, and D. J. Maitland, "Shape memory polyurethanes with oxidation-induced degradation: In vivo and in vitro correlations for endovascular material applications," *Acta Biomaterialia*, Vol. 59, pp. 33–44, Sept. 2017.

43. Ruan, C., Y. Wang, M. Zhang, Y. Luo, C. Fu, M. Huang, J. Sun, and C. Hu, "Design, synthesis and characterization of novel biodegradable shape memory polymers based on poly(D , L -lactic acid) diol, hexamethylene diisocyanate and piperazine: Novel biodegradable shape memory polymers," *Polymer International*, Vol. 61, pp. 524–530, Apr. 2012.

44. Hu, N., C. Ruan, X. Ning, and C. Xu, "Design, Synthesis and Characterization of Novel Biodegradable Poly(urethane-urea) for Biomedical Applications," *Asian Journal of Chemistry*, Vol. 25, no. 8, pp. 4327–4330, 2013.

45. Ruan, C., Y. Hu, L. Jiang, Q. Cai, H. Pan, and H. Wang, "Tunable degradation of piperazine-based polyurethane ureas," *Journal of Applied Polymer Science*, Vol. 131, pp. n/a–n/a, Oct. 2014.

46. Ruan, C., N. Hu, Y. Hu, L. Jiang, Q. Cai, H. Wang, H. Pan, W. W. Lu, and Y. Wang, "Piperazine-based polyurethane-ureas with controllable degradation as potential bone scaffolds," *Polymer*, Vol. 55, pp. 1020–1027, Feb. 2014.

47. Xie, H., J. Shao, Y. Ma, J. Wang, H. Huang, N. Yang, H. Wang, C. Ruan, Y. Luo, Q.-Q. Wang, P. K. Chu, and X.-F. Yu, "Biodegradable near-infrared-photoresponsive shape memory implants based on black phosphorus nanofillers," *Biomaterials*, Vol. 164, pp. 11–21, May 2018.

48. Shi, S., Q.-Y. Wu, L. Gu, K. Zhang, and H. Yu, "Bio-based (co)polylactide-urethane networks with shape memory behavior at body temperature," *RSC Advances*, Vol. 6, no. 83, pp. 79268–79274, 2016.

49. Luo, Q., J. Chen, P. Gnanasekar, X. Ma, D. Qin, H. Na, J. Zhu, and N. Yan, "A facile preparation strategy of polycaprolactone (PCL)-based biodegradable polyurethane elastomer with a highly efficient shape memory effect," *New Journal of Chemistry*, Vol. 44, no. 3, pp. 658–662, 2020.

50. Wang, Y., P. Zhang, Y. Zhao, R. Dai, M. Huang, W. Liu, H. Liu, S. He, and C. Zhu, "Shape memory composites composed of polyurethane/ZnO nanoparticles as potential smart biomaterials," *Polymer Composites*, Vol. 41, pp. 2094–2107, May 2020.

51. Bil, M., E. Kijeńska-Gawrońska, E. Głodkowska-Mrówka, A. Manda-Handzlik, and P. Mrówka, "Design and in vitro evaluation of electrospun shape memory polyurethanes for self-fitting tissue engineering grafts and drug delivery systems," *Materials Science and Engineering: C*, Vol. 110, p. 110675, May 2020.

52. Eyvazzadeh Kalajahi, A., M. Rezaei, and F. Abbasi, "Preparation, characterization, and thermo-mechanical properties of poly (ε-caprolactone)-piperazine-based polyurethane-urea shape memory polymers," *Journal of Materials Science*, Vol. 51, pp. 4379–4389, May 2016.

53. Wu, L., C. Jin, and X. Sun, "Synthesis, Properties, and Light-Induced Shape Memory Effect of Multiblock Polyesterurethanes Containing Biodegradable Segments and Pendant Cinnamamide Groups," *Biomacromolecules*, Vol. 12, pp. 235–241, Jan. 2011.

54. Ramezani, M., and M. B. B. Monroe, "Biostable Segmented Thermoplastic Polyurethane Shape Memory Polymers for Smart Biomedical Applications," *ACS Applied Polymer Materials*, Vol. 4, pp. 1956–1965, Mar. 2022.

55. Gupta, A., and T. H. Mekonnen, "Cellulose nanocrystals enabled sustainable polycaprolactone based shape memory polyurethane bionanocomposites," *Journal of Colloid and Interface Science*, Vol. 611, pp. 726–738, Apr. 2022.

56. Gu, L., B. Cui, Q.-Y. Wu, and H. Yu, "Bio-based polyurethanes with shape memory behavior at body temperature: effect of different chain extenders," *RSC Advances*, Vol. 6, no. 22, pp. 17888–17895, 2016.

57. Cui, B., Q.-Y. Wu, L. Gu, L. Shen, and H.-b. Yu, "High performance bio-based polyurethane elastomers: Effect of different soft and hard segments," *Chinese Journal of Polymer Science*, Vol. 34, pp. 901–909, July 2016.

58. Shaabani, A., R. Sedghi, H. Motasadizadeh, and R. Dinarvand, "Self-healable conductive polyurethane with the body temperature-responsive shape memory for bone tissue engineering," *Chemical Engineering Journal*, Vol. 411, p. 128449, May 2021.

59. Shaabani, A., and R. Sedghi, "Synthesis of shape memory electroconductive polyurethane with self-healing capability as an intelligent biomedical scaffold for bone tissue engineering," *Polymer*, Vol. 223, p. 123694, May 2021.

60. Mehrbakhsh, E., M. Rezaei, R. Lotfi Mayan Sofla, and A. Babaie, "Physical and thermo-mechanical properties of PCL/PEG based shape memory polyurethane for orthodontic ligature application," *International Journal of Polymeric Materials and Polymeric Biomaterials*, pp. 1–11, Dec. 2022.

61. Wang, L., X. Yang, H. Chen, T. Gong, W. Li, G. Yang, and S. Zhou, "Design of Triple-Shape Memory Polyurethane with Photo-cross-linking of Cinnamon Groups," *ACS Applied Materials & Interfaces*, Vol. 5, pp. 10520–10528, Nov. 2013.

62. Yang, X., L. Wang, W. Wang, H. Chen, G. Yang, and S. Zhou, "Triple Shape Memory Effect of Star-Shaped Polyurethane," *ACS Applied Materials & Interfaces*, Vol. 6, pp. 6545–6554, May 2014.

63. Ahmad, M., J. Luo, B. Xu, H. Purnawali, P. J. King, P. R. Chalker, Y. Fu, W. Huang, and M. Miraftab, "Synthesis and Characterization of Polyurethane-Based Shape-Memory Polymers for Tailored T_g around Body Temperature for Medical Applications: Synthesis and Characterization of Polyurethane-Based Shape-Memory ...," *Macromolecular Chemistry and Physics*, Vol. 212, pp. 592–602, Mar. 2011.

64. Wang, L., X. Yang, H. Chen, G. Yang, T. Gong, W. Li, and S. Zhou, "Multi-stimuli sensitive shape memory poly(vinyl alcohol)-graft-polyurethane," *Polymer Chemistry*, Vol. 4, no. 16, p. 4461, 2013.

65. Ansari, M., M. Golzar, M. Baghani, and M. Soleimani, "Shape memory characterization of poly(ε-caprolactone) (PCL)/polyurethane (PU) in combined torsion-tension loading with potential applications in cardiovascular stent," *Polymer Testing*, Vol. 68, pp. 424–432, July 2018.

66. Sivakumar, C., and A. S. Nasar, "Poly(ε-caprolactone)-based hyperbranched polyurethanes prepared via A2+B3 approach and its shape-memory behavior," *European Polymer Journal*, Vol. 45, pp. 2329–2337, Aug. 2009.

67. Sabahi, N., I. Roohani, C. H. Wang, E. Farajzadeh, and X. Li, "Thermoplastic polyurethane-based shape memory polymers with potential biomedical application: The effect of TPU soft-segment on shape memory effect and cytocompatibility," *Polymer*, Vol. 283, p. 126189, Sept. 2023.

68. Zhang, Y., C. Li, W. Zhang, J. Deng, Y. Nie, X. Du, L. Qin, and Y. Lai, "3D-printed NIR-responsive shape memory polyurethane/magnesium scaffolds with tight-contact for robust bone regeneration," *Bioactive Materials*, Vol. 16, pp. 218–231, Oct. 2022.

69. Mo, F., F. Zhou, S. Chen, H. Yang, Z. Ge, and S. Chen, "Development of shape memory polyurethane based on polyethylene glycol and liquefied 4,4'-diphenylmethane diisocyanate using a bulk method for biomedical applications: PEG6000 based shape memory polyurethane," *Polymer International*, Vol. 64, pp. 477–485, Apr. 2015.

70. Cui, J., K. Kratz, M. Heuchel, B. Hiebl, and A. Lendlein, "Mechanically active scaffolds from radio-opaque shape-memory polymer-based composites," *Polymers for Advanced Technologies*, Vol. 22, pp. 180–189, Jan. 2011.

71. Sarkar, D., J.-C. Yang, and S. T. Lopina, "Structure-property relationship ofL-tyrosine-based polyurethanes for biomaterial applications," *Journal of Applied Polymer Science*, Vol. 108, pp. 2345–2355, May 2008.

72. Sarkar, D., J.-C. Yang, A. S. Gupta, and S. T. Lopina, "Synthesis and characterization of L-tyrosine based polyurethanes for biomaterial applications," *Journal of Biomedical Materials Research Part A*, Vol. 90A, pp. 263–271, June 2009.

73. Dou, H.-M., J.-H. Ding, H. Chen, Z. Wang, A.-F. Zhang, and H.-B. Yu, "Bio-based, biodegradable and amorphous polyurethanes with shape memory behavior at body temperature," *RSC Advances*, Vol. 9, no. 23, pp. 13104–13111, 2019.

74. Ping, P., W. Wang, X. Chen, and X. Jing, "Poly(ε-caprolactone) Polyurethane and Its Shape-Memory Property," *Biomacromolecules*, Vol. 6, pp. 587–592, Mar. 2005.

75. Gnavi, S., C. Barwig, T. Freier, K. Haastert-Talini, C. Grothe, and S. Geuna, "The Use of Chitosan-Based Scaffolds to Enhance Regeneration in the Nervous System," in *International Review of Neurobiology*, Vol. 109, pp. 1–62, Elsevier, 2013.

76. Tajvar, S., A. Hadjizadeh, and S. S. Samandari, "Scaffold degradation in bone tissue engineering: An overview," *International Biodeterioration & Biodegradation*, Vol. 180, p. 105599, May 2023.

77. Staiger, M. P., A. M. Pietak, J. Huadmai, and G. Dias, "Magnesium and its alloys as orthopedic biomaterials: A review," *Biomaterials*, Vol. 27, pp. 1728–1734, Mar. 2006.

78. Huiskes, R., H. Weinans, and B. V. Rietbergen, "The Relationship Between Stress Shielding and Bone Resorption Around Total Hip Stems and the Effects of Flexible Materials:," *Clinical Orthopaedics and Related Research*, Vol. 274, p. 124???134, Jan. 1992.

79. Su, S., and P. M. Kang, "Systemic Review of Biodegradable Nanomaterials in Nanomedicine," *Nanomaterials*, Vol. 10, p. 656, Apr. 2020.

80. Borhani, S., S. Hassanajili, S. H. Ahmadi Tafti, and S. Rabbani, "Cardiovascular stents: overview, evolution, and next generation," *Progress in Biomaterials*, Vol. 7, pp. 175–205, Sept. 2018.

81. Lee, J., and S.-K. Kang, "Principles for Controlling the Shape Recovery and Degradation Behavior of Biodegradable Shape-Memory Polymers in Biomedical Applications," *Micromachines*, Vol. 12, p. 757, June 2021.

82. Nguyen, T. P. T., C. Ménager, J. Rieger, and F. Coumes, "Rational design of stimuli-responsive magnetic polymer hybrid (nano)materials," *Polymer International*, Vol. 72, pp. 899–919, Oct. 2023.

83. Lee, J. H., E. D. Kim, E. J. Jun, H. S. Yoo, and J. W. Lee, "Analysis of trends and prospects regarding stents for human blood vessels," *Biomaterials Research*, Vol. 22, p. 8, Dec. 2018.

84. Tang, A. Y.-S., H.-N. Chan, A. C.-O. Tsang, G. K.-K. Leung, K.-M. Leung, A. C.-H. Yu, and K.-W. Chow, "The effects of stent porosity on the endovascular treatment of intracranial aneurysms located near a bifurcation," *Journal of Biomedical Science and Engineering*, Vol. 06, no. 08, pp. 812–822, 2013.

85. Baer, G. M., T. S. Wilson, W. Small, J. Hartman, W. J. Benett, D. L. Matthews, and D. J. Maitland, "Thermomechanical properties, collapse pressure, and expansion of shape memory polymer neurovascular stent prototypes," *Journal of Biomedical Materials Research Part B: Applied Biomaterials*, Vol. 90B, pp. 421–429, Dec. 2008.

86. Bellin, I., S. Kelch, R. Langer, and A. Lendlein, "Polymeric triple-shape materials," *Proceedings of the National Academy of Sciences*, Vol. 103, pp. 18043–18047, Nov. 2006.

87. Yakacki, C. M., R. Shandas, C. Lanning, B. Rech, A. Eckstein, and K. Gall, "Unconstrained recovery characterization of shape-memory polymer networks for cardiovascular applications," *Biomaterials*, Vol. 28, pp. 2255–2263, May 2007.

88. Yang, C.-S., H.-C. Wu, J.-S. Sun, H.-M. Hsiao, and T.-W. Wang, "Thermo-Induced Shape-Memory PEG-PCL Copolymer as a Dual-Drug-Eluting Biodegradable Stent," *ACS Applied Materials & Interfaces*, Vol. 5, pp. 10985–10994, Nov. 2013.

89. Venkatraman, S. S., L. P. Tan, J. F. D. Joso, Y. C. F. Boey, and X. Wang, "Biodegradable stents with elastic memory," *Biomaterials*, Vol. 27, pp. 1573–1578, Mar. 2006.

90. Chen, M.-C., H.-W. Tsai, Y. Chang, W.-Y. Lai, F.-L. Mi, C.-T. Liu, H.-S. Wong, and H.-W. Sung, "Rapidly Self-Expandable Polymeric Stents with a Shape-Memory Property," *Biomacromolecules*, Vol. 8, pp. 2774–2780, Sept. 2007.

91. Xue, L., S. Dai, and Z. Li, "Biodegradable shape-memory block co-polymers for fast self-expandable stents," *Biomaterials*, Vol. 31, pp. 8132–8140, Nov. 2010.

92. Rodriguez, J. N., W. Hwang, J. Horn, T. L. Landsman, A. Boyle, M. A. Wierzbicki, S. M. Hasan, D. Follmer, J. Bryant, W. Small, and D. J. Maitland, "Design and biocompatibility of endovascular aneurysm filling devices: ENDOVASCULAR ANEURYSM FILLING DEVICES," *Journal of Biomedical Materials Research Part A*, Vol. 103, pp. 1577–1594, Apr. 2015.

93. Lazareska, M., V. Aliji, E. Stojovska-Jovanovska, J. Businovska, V. Mircevski, M. Kostov, and M. Papazova, "Endovascular Treatment of Wide Neck Aneurysms," *Open Access Macedonian Journal of Medical Sciences*, Vol. 6, pp. 2316–2322, Dec. 2018.

94. Hampikian, J. M., B. C. Heaton, F. C. Tong, Z. Zhang, and C. Wong, "Mechanical and radiographic properties of a shape memory polymer composite for intracranial aneurysm coils," *Materials Science and Engineering: C*, Vol. 26, pp. 1373–1379, Sept. 2006.

95. Metcalfe, A., A.-C. Desfaits, I. Salazkin, L. Yahia, W. M. Sokolowski, and J. Raymond, "Cold hibernated elastic memory foams for endovascular interventions," *Biomaterials*, Vol. 24, pp. 491–497, Feb. 2003.

96. Baker, R. M., J. H. Henderson, and P. T. Mather, "Shape memory poly(ε-caprolactone)-co-poly(ethylene glycol) foams with body temperature triggering and two-way actuation," *Journal of Materials Chemistry B*, Vol. 1, no. 38, p. 4916, 2013.

97. Small, W., P. R. Buckley, T. S. Wilson, W. J. Benett, J. Hartman, D. Saloner, and D. J. Maitland, "Shape Memory Polymer Stent With Expandable Foam: A New Concept for Endovascular Embolization of Fusiform Aneurysms," *IEEE Transactions on Biomedical Engineering*, Vol. 54, pp. 1157–1160, June 2007.

98. Metzger, M. F., T. S. Wilson, D. Schumann, D. L. Matthews, and D. J. Maitland, "Mechanical Properties of Mechanical Actuator for Treating Ischemic Stroke," *Biomedical Microdevices*, Vol. 4, no. 2, pp. 89–96, 2002.

99. Small IV, W., T. S. Wilson, W. J. Benett, J. M. Loge, and D. J. Maitland, "Laser-activated shape memory polymer intravascular thrombectomy device," *Optics Express*, Vol. 13, p. 8204, Oct. 2005.

100. Small, W., T. S. Wilson, P. R. Buckley, W. J. Benett, J. M. Loge, J. Hartman, and D. J. Maitland, "Prototype Fabrication and Preliminary *In Vitro* Testing of a Shape Memory Endovascular Thrombectomy Device," *IEEE Transactions on Biomedical Engineering*, Vol. 54, pp. 1657–1666, Sept. 2007.

101. Wang, K., Y.-G. Jia, C. Zhao, and X. Zhu, "Multiple and two-way reversible shape memory polymers: Design strategies and applications," *Progress in Materials Science*, Vol. 105, p. 100572, Aug. 2019.

102. Wang, Y., X. Pei, Q. Pei, Z. Zhang, Y. Zhang, Q. Wang, and T. Wang, "Shape memory polylactic acid/modified *Eucommia ulmoides* gum thermoplastic vulcanizates based on excellent interfacial adhesion and co-continuous structure," *Polymer International*, Vol. 73, pp. 435–445, June 2024.

103. Tang, Z., Y. Chen, C. Zhang, S. Wu, B. Guo, and L. Zhang, "Dual dynamic crosslinking of rubber for enhanced mechanical properties and reconfigurable shape memory behavior," *Polymer International*, Vol. 72, pp. 783–789, Sept. 2023.

104. Costanza, G., and M. E. Tata, "Shape Memory Alloys for Aerospace, Recent Developments, and New Applications: A Short Review," *Materials*, Vol. 13, p. 1856, Apr. 2020.

105. Chan, B. Q. Y., Z. W. K. Low, S. J. W. Heng, S. Y. Chan, C. Owh, and X. J. Loh, "Recent Advances in Shape Memory Soft Materials for Biomedical Applications," *ACS Applied Materials & Interfaces*, Vol. 8, pp. 10070–10087, Apr. 2016.

106. Wei, Z. G., R. Sandstroröm, and S. Miyazaki, "Shape-memory materials and hybrid composites for smart systems: Part I Shape-memory materials," *Journal of Materials Science*, Vol. 33, no. 15, pp. 3743–3762, 1998.

107. Zhang, N., and M. Asle Zaeem, "Nanoscale self-healing mechanisms in shape memory ceramics," *npj Computational Materials*, Vol. 5, p. 54, May 2019.

108. Fadlallah, S. A., N. El-Bagoury, S. M. Gad El-Rab, R. A. Ahmed, and G. El-Ousamii, "An overview of NiTi shape memory alloy: Corrosion resistance and antibacterial inhibition for dental application," *Journal of Alloys and Compounds*, Vol. 583, pp. 455–464, Jan. 2014.

109. Shayanfard, P., F. Wendler, P. Hempel, and M. Karl, "Design and Numerical-Method-Aided Optimization of a Novel Attachment System for Implant-Retained Dental Prostheses Using NiTi Shape Memory Alloys," *Applied Sciences*, Vol. 13, p. 491, Dec. 2022.

110. Peterson, G. I., A. V. Dobrynin, and M. L. Becker, "Biodegradable Shape Memory Polymers in Medicine," *Advanced Healthcare Materials*, Vol. 6, p. 1700694, Nov. 2017.

111. Yang, R., W. Liu, A. Wang, X. Deng, Y. Feng, Q. Zhang, Z. Li, F. Luo, J. Li, and H. Tan, "Shape memory polyurethane potentially used for vascular stents with water-induced stiffening and improved hemocompatibility," *Journal of Materials Chemistry B*, Vol. 10, no. 43, pp. 8918–8930, 2022.

112. Wierzbicki, M. A., J. Bryant, M. W. Miller, B. Keller, and D. J. Maitland, "Mechanical and in vitro evaluation of an experimental canine patent ductus arteriosus occlusion device," *Journal of the Mechanical Behavior of Biomedical Materials*, Vol. 59, pp. 156–167, June 2016.

113. Horn, J., W. Hwang, S. L. Jessen, B. K. Keller, M. W. Miller, E. Tuzun, J. Hartman, F. J. Clubb, and D. J. Maitland, "Comparison of shape memory polymer foam versus bare metal coil treatments in an *in vivo* porcine sidewall aneurysm model: COMPARISON OF SHAPE MEMORY POLYMER FOAM VERSUS BARE METAL COIL TREATMENTS," *Journal of Biomedical Materials Research Part B: Applied Biomaterials*, Vol. 105, pp. 1892–1905, Oct. 2017.

114. Landsman, T. L., R. L. Bush, A. Glowczwski, J. Horn, S. L. Jessen, E. Ungchusri, K. Diguette, H. R. Smith, S. M. Hasan, D. Nash, F. J. Clubb, and D. J. Maitland, "Design and verification of a shape memory polymer peripheral occlusion device," *Journal of the Mechanical Behavior of Biomedical Materials*, Vol. 63, pp. 195–206, Oct. 2016.

115. Jessen, S. L., M. C. Friedemann, A.-M. Ginn-Hedman, L. M. Graul, S. Jokerst, C. B. Robinson, T. L. Landsman, F. J. Clubb, and D. J. Maitland, "Microscopic Assessment of Healing and Effectiveness of a Foam-Based Peripheral Occlusion Device," *ACS Biomaterials Science & Engineering*, Vol. 6, pp. 2588–2599, May 2020.

116. Hasan, S. M., G. K. Fletcher, M. B. B. Monroe, M. A. Wierzbicki, L. D. Nash, and D. J. Maitland, "Shape Memory Polymer Foams Synthesized Using Glycerol and Hexanetriol for Enhanced Degradation Resistance," *Polymers*, Vol. 12, p. 2290, Oct. 2020.

117. Weems, A. C., K. T. Wacker, and D. J. Maitland, "Improved oxidative biostability of porous shape memory polymers by substituting triethanolamine for glycerol," *Journal of Applied Polymer Science*, Vol. 136, p. 47857, Sept. 2019.

118. Lendlein, A., S. Kelch, K. Kratz, J. Schulte, and S. Schauer, "Shape-Memory Polymers," in *Reference Module in Materials Science and Materials Engineering*, p. B9780128035818092444, Elsevier, 2016.

119. Ur Rehman, H., Y. Chen, M. S. Hedenqvist, H. Li, W. Xue, Y. Guo, Y. Guo, H. Duan, and H. Liu, "Self-Healing Shape Memory PUPCL Copolymer with High Cycle Life," *Advanced Functional Materials*, Vol. 28, p. 1704109, Feb. 2018.

120. Zhang, L., H. K. Jeon, J. Malsam, R. Herrington, and C. W. Macosko, "Substituting soybean oil-based polyol into polyurethane flexible foams," *Polymer*, Vol. 48, pp. 6656–6667, Oct. 2007.

121. Yılgör, E., I. Yılgör, and E. Yurtsever, "Hydrogen bonding and polyurethane morphology. I. Quantum mechanical calculations of hydrogen bond energies and vibrational spectroscopy of model compounds," *Polymer*, Vol. 43, pp. 6551–6559, Nov. 2002.

122. Achorn, P. J., and R. G. Ferrillo, "Comparison of thermal techniques for glass transition measurements of polystyrene and cross-linked acrylic polyurethane films," *Journal of Applied Polymer Science*, Vol. 54, pp. 2033–2043, Dec. 1994.

123. Bandeira, C. F., S. R. Montoro, E. L. Espindola, E. C. Botelho, M. L. Costa, and M. O. H. Cioffi, "Comparison of Glass Transition Temperature Values of Composite Polymer Obtained by TMA and DSC," *Applied Mechanics and Materials*, Vol. 719-720, pp. 91–95, Jan. 2015.

124. Backfolk, K., R. Holmes, P. Ihalainen, P. Sirviö, N. Triantafillopoulos, and J. Peltonen, "Determination of the glass transition temperature of latex films: Comparison of various methods," *Polymer Testing*, Vol. 26, pp. 1031–1040, Dec. 2007.

125. Yong, A. X. H., G. D. Sims, S. J. P. Gnaniah, S. L. Ogin, and P. A. Smith, "Heating rate effects on thermal analysis measurement of T_g in composite materials," *Advanced Manufacturing: Polymer & Composites Science*, Vol. 3, pp. 43–51, Apr. 2017.

126. Startsev, O. V., Y. M. Vapirov, M. P. Lebedev, and A. K. Kychkin, "Comparison of Glass-Transition Temperatures for Epoxy Polymers Obtained by Methods of Thermal Analysis," *Mechanics of Composite Materials*, Vol. 56, pp. 227–240, May 2020.

127. Fan, Q., and C. Xiao, "Effects of crosslinking density on structure and properties of interpenetrating polymer networks from polyurethane and nitroguar gum," *Polymer Composites*, Vol. 29, pp. 758–767, July 2008.

128. Cannella, V., R. Altomare, G. Chiaramonte, S. Di Bella, F. Mira, L. Russotto, P. Pisano, and A. Guercio, "Cytotoxicity Evaluation of Endodontic Pins on L929 Cell Line," *BioMed Research International*, Vol. 2019, pp. 1–5, Oct. 2019.

129. Hancock, B. C., and G. Zografi, "The relationship between the glass transition temperature and the water content of amorphous pharmaceutical solids," *Pharmaceutical Research*, Vol. 11, no. 4, pp. 471–477, 1994.

130. Garces, I., S. Aslanzadeh, Y. Boluk, and C. Ayranci, "Effect of Moisture on Shape Memory Polyurethane Polymers for Extrusion-Based Additive Manufacturing," *Materials*, Vol. 12, p. 244, Jan. 2019.

131. Yang, B., W. Huang, C. Li, and L. Li, "Effects of moisture on the thermomechanical properties of a polyurethane shape memory polymer," *Polymer*, Vol. 47, pp. 1348–1356, Feb. 2006.

132. Yu, Y.-J., K. Hearon, T. S. Wilson, and D. J. Maitland, "The effect of moisture absorption on the physical properties of polyurethane shape memory polymer foams," *Smart Materials and Structures*, Vol. 20, p. 085010, Aug. 2011.

133. Wang, H., C. Dong, P. Zhao, S. Wang, Z. Liu, and J. Chang, "Lipid coated upconverting nanoparticles as NIR remote controlled transducer for simultaneous photodynamic therapy and cell imaging," *International Journal of Pharmaceutics*, Vol. 466, pp. 307–313, May 2014.

134. Majaron, B., and J. S. Nelson, "Laser Treatment of Port Wine Stains," in *Optical-Thermal Response of Laser-Irradiated Tissue* (Welch, A. J., and M. J. van Gemert, eds.), pp. 859–913, Dordrecht: Springer Netherlands, 2010.

135. Sienkiewicz, Z., E. Van Rongen, R. Croft, G. Ziegelberger, and B. Veyret, "A Closer Look at the Thresholds of Thermal Damage: Workshop Report by an ICNIRP Task Group," *Health Physics*, Vol. 111, pp. 300–306, Sept. 2016.

136. Yarmolenko, P. S., E. J. Moon, C. Landon, A. Manzoor, D. W. Hochman, B. L. Viglianti, and M. W. Dewhirst, "Thresholds for thermal damage to normal tissues: An update," *International Journal of Hyperthermia*, Vol. 27, pp. 320–343, June 2011.

137. Morton, A. C., D. Crossman, and J. Gunn, "The influence of physical stent parameters upon restenosis," *Pathologie Biologie*, Vol. 52, pp. 196–205, May 2004.

138. Li, Z., and C. Kleinstreuer, "Analysis of biomechanical factors affecting stent-graft migration in an abdominal aortic aneurysm model," *Journal of Biomechanics*, Vol. 39, pp. 2264–2273, Jan. 2006.

139. "ISO 10993-1:2018," 2018.